

## A review of experimental and numerical investigations about crack propagation

Vahab Sarfarazi<sup>1</sup> and Hadi Haeri<sup>\*2</sup>

<sup>1</sup>Department of Mining Engineering, Hamedan University of Technology, Hamedan, Iran

<sup>2</sup>Department of Mining Engineering, Bafgh Branch, Islamic Azad University, Bafgh, Iran

(Received February 15, 2016, Revised April 13, 2016, Accepted April 19, 2016)

**Abstract.** A rock mass containing non-persistent joints can only fail if the joints propagate and coalesce through an intact rock bridge. Shear strength of rock mass containing non-persistent joints is highly affected by the both, mechanical behavior and geometrical configuration of non-persistent joints located in a rock mass. Existence of rock joints and rock bridges are the most important factors complicating mechanical responses of a rock mass to stress loading. The joint-bridge interaction and bridge failure dominates mechanical behavior of jointed rock masses and the stability of rock excavations. The purpose of this review paper is to present techniques, progresses and the likely future development directions in experimental and numerical modelling of a non-persistent joint failure behaviour. Such investigation is essential to study the fundamental failures occurring in a rock bridge, for assessing anticipated and actual performances of the structures built on or in rock masses. This paper is divided into two sections. In the first part, experimental investigations have been represented followed by a summarized numerical modelling. Experimental results showed failure mechanism of a rock bridge under different loading conditions. Also effects of the number of non-persistent joints, angle between joint and a rock bridge, lengths of the rock bridge and the joint were investigated on the rock bridge failure behaviour. Numerical simulation results are used to validate experimental outputs.

**Keywords:** non-persistent joint; experimental test; numerical simulation

---

### 1. Introduction

Lengths of the fractures in natural rocks can vary from tens of kilometres down to tens of microns. In addition, the joints in rocks are normally discontinuous in nature with limited lengths. There are only few cases where the cause and the location of failure in rock structure limited to a single discontinuity. Usually, several discontinuities of limited size interact and eventually form a combined shear plane where the failure takes place (Committee on Fracture Characterization and Fluid Flow 1996). So, besides the discontinuities themselves, regions between adjacent discontinuities consisting strong rock which called the rock bridges are of utmost importance for the shear strength of compound failure plane (Jaeger 1971, Einstein *et al* 1983). From the practical

---

\*Corresponding author, Assistant Professor, E-mail: haerihadi@gmail.com

point of view and to a certain extent, in nearly all rock engineering projects, constructions of structures in or on rock masses contain both; fractures and rock bridges. The crack coalescence in a rock bridge is usually responsible for the failure of many rock structures. Also, higher strength of rock mass is mainly induced by the presence and the arrangement of rock bridges (Stimpson 1978, Jennings 1970, Zhao 1995, Horii *et al* 1986). One claims to be on the safe side since the rock bridges are thought to produce a strength reserve, as they have to be broken first before failure can take place along the newly separated plane (Stimpson 1978). In some approaches, the rock bridges are taken to be responsible for increasing additional cohesive strength (Einstein *et al* 1983, Stimpson 1978, Jennings 1970).

From other point of views, the collapse of underground structures can be regarded as either; the movement of fractured block in fully persistent jointed rock masses, or propagation and coalescence of non-persistent joints around excavation surface. Therefore, the mechanism of crack coalescence in the rock bridge area between pre-existing joints remains one of the most fundamental theoretical problems in rock mechanics to be solved. A comprehensive study on the shear failure behaviour of jointed rock can provide a good understanding of local and general rock instabilities, leading to improved designs for the rock engineering projects. In the following sections, experimental and numerical studies will be described.

## 2. Experimental analyses

Crack initiation and propagation have been the subjects of intensive investigations in rock mechanics, both theoretically and experimentally. First theoretical study on growth of the pre-existing two-dimensional cracks was given by Griffith (1921, 1924). Irwin (1957) further introduced the concept of critical energy release rate and the crack tip stress intensity factor ( $K$ ). With respect to the field of rock mechanics, a number of experimental studies have been carried out to investigate the crack initiation, propagation and interaction (Hoek *et al.* 1965, Pang *et al.* 1972, Hallbaue *et al.* 1973, Tapponn *et al.* 1976, Olsson *et al.* 1976, Kranz 1983, Batzle *et al.* 1980, Wong 1982; Pan *et al.*, 2014; Haeri *et al.*, 2014a, 2014b, 2014c, 2014d, 2014e, 2014f; Ibraheem *et al.*, 2015; Haeri *et al.*, 2015a, 2015b, Haeri, 2015c, 2015d, 2015e; Haeri and Sarfarazi, 2016a, 2016b). For a comprehensive literature review on micro-crack studies, it refers to Kranz (1983). Meanwhile, many mathematical models were developed to explain and predict the processes of crack growth, interaction and rock failure (Dey *et al.* 1981, Steif 1984, Horii *et al.* 1985, Ashby *et al.* 1986, Sammis *et al.* 1986, Kemeny *et al.* 1987, Kemeny 1991). For discussing on how these shear crack models can be applied to real rocks, it refers to the comparative study by Fredrich *et al.* (1990).

A number of researches were described their studies on crack propagation on different materials in uniaxial compression forms (Nemat-Nasser & Horii 1982, Hoek & Bieniawski 1984, Jiefan *et al.* 1990). A common crack pattern found in rocks and rock-model materials under compressive loading was also summarized by Bobet (2000) as follows (see Fig. 1): 1. Wing cracks start at the tips of the fractures and propagate in a curvilinear path as load increases. Wing cracks as the tensile type grow in stable manner, since an increase in loading is necessary to lengthen the cracks. Wing cracks tend to align with the direction of the most compressive stress. 2. Secondary cracks are generally described as shear cracks or shear zones. They initiate from the tips of the fractures and there two directions are possible: (1) coplanar or nearly coplanar to the fractures; (2) with an inclination similar to wing cracks but in opposite direction.

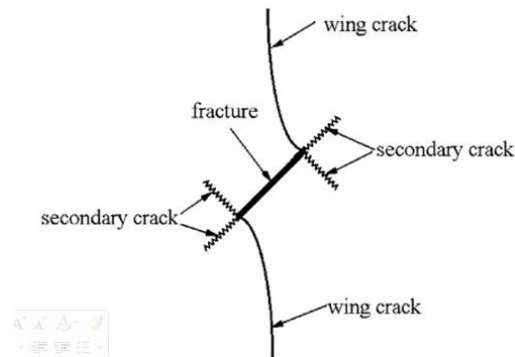


Fig. 1 A common crack pattern found in rocks and rock-model materials, Bobet (2000)

Ingrafea and Heuze (1980) observed similar crack pattern in uniaxial compression tests on limestone and grano diorite specimens with single inclined flaws. Petit and Barquins (1988) studied crack propagation in sandstone from a single flaw subjected to uniaxial compression; tensile cracks, or “Branch Fractures”, and a “Shear Zone” were observed at the tips of the flaw. Chen *et al.* (1992) conducted uniaxial experiments on marble; first, tensile cracks appeared near and at the tip of the flaw. As the load was increased, an “X” shape band appeared at and extended from the tips of the flaw approaching to the specimen boundary. A number of investigators have reported cracks with similar characteristics in the specimens containing single inclined flaw (Einstein *et al.* 1993, Pang *et al.* 1972, Hallbauer 1973, Tapponnier *et al.* 1976, Olsson *et al.* 1976, Kranz 1979, Batzle *et al.* 1980, Dey *et al.* 1981, Germanovich 1996, Steif 1984, Sagong *et al.* 2000, Bieniawski 1967, Jamil 1999, Alzo’ubi 2001, Bobet 1997, Bobet *et al.* 1998, Celestino *et al.* 2001, Huang *et al.* 1999, Li *et al.* 2003, Papadopoulos *et al.* 1983, Shah 1999a, Shah 1999b, Shang 1999, Shen 1993, Shen *et al.* 1995, Tang *et al.* 1998, Takeuchi 1991, Wong *et al.* 1998, Deng *et al.* 1984, Zhu *et al.* 1998; Haeri *et al.*, 2014a, 2014b; Haeri *et al.*, 2015a, 2015b, Haeri, 2015c, 2015d; Haeri and Sarfarazi, 2016a, 2016b).

Reyes (1991), Shah (1999 a,b), Shen (1993, 1995), Bobet (1997), Bobet and Einstein (1998), Zhu *et al.* (1998), Wong and Chau (1998) and Wong *et al.* (1997) have investigated crack propagation and coalescence on rock-like materials specimens containing two inclined flaws which both were either open or closed. Besides model materials, real rock samples are also employed to study the rock materials with fractures. Examples include the work of Huang *et al.* (1999) and Celestino *et al.* (2001) on marble and Shang *et al.* (1999) on granite and marble. They found that wing cracks and secondary cracks (initiating after the wing cracks) may occur and eventually lead to coalescence under uniaxial compression. To incorporate the effect of crack surface friction, Shen *et al.* (1993) conducted a series of uniaxial compressive tests on gypsum specimens containing both, open and closed fractures. It was found that the initial geometrical setting of parallel flaws controls the mechanism of crack coalescence. The observed patterns of crack coalescence were similar to those reported in the study by Wong and Chau (1998). Failure of flawed solids may occur in tensile and/or shear modes, depending on geometrical relation between the two pre-existing flaws. Based upon the experimental work by Wong and Chau (1998) and Shen *et al.* (1995), Wong and Chau (1997) reconsidered the problems of crack coalescence and the strength between the two flaws by using a rock-like material (made of barite, sand, plaster and water) under uniaxial compression. Three main factors were changed to investigate the failure

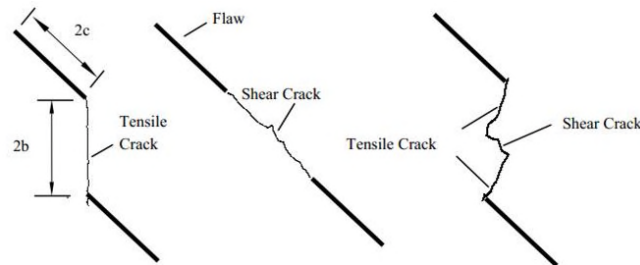


Fig. 2 three main modes of crack coalescence Wong and Chau (1998)

patterns: the flaw angle ' $\alpha$ ' (inclination of the flaw), the bridge angle ' $\beta$ ' (angle between two flaws) and the frictional coefficient ' $\mu$ ' of flaw surface, under the conditions of a fixed flaw length ' $2c$ ' and a fixed distance between the flaws ' $2b$ '. In general, three main modes of crack coalescence were observed as shown in Fig. 2. They are the wing tensile mode (crack coalescence involving the growth of wing cracks along the direction parallel to the compression), the shear mode (links between two flaws along the direction roughly parallel to the flaw), and the mixed mode (shear/tensile). Wong and Chau (1998) proposed a classification of patterns for three different failure modes (tensile, shear and mixed), for different combinations of flaw angle  $\alpha$ ; bridge angle  $\beta$  and frictional coefficient  $\mu$  on flaw surface.

Wong (1997), Wong *et al.* (1997, 1998) and Wong and Chau (1998) found that compressive strength of specimen for the wing crack coalescence is normally lower than that for the shear crack coalescence. Furthermore, Wong and Chau (1998) found that the strength of cracked solids does not show any linear relation with the number of pre-existing flaws (density) once a threshold value of flaw density is exceeded. In those researches, the effect of confining pressure on crack growth properties has eliminated.

Model tests have been conducted to study the effect of structural planes on the deformation characterizes of rocks by Hu *et al.* 2009, and the strength computing method of rock with intermittent joints is proposed. The deformation characterizes of rocks contain structural planes are analyzed by Mao *et al.* 2009.

Hall *et al.* (2006) has investigated the fracture propagation in a soft rock consisting imbedded non-persistent joint using acoustic emissions and digital images.

Based on the observations made, for tuff Neapolitan fine-grained, failure is highly dependent on the juxtaposition of the flaws. As such, a general description of the fracture development and coalescence in the rock bridge has been identified with three phases similar to that in a classical form. Few precursory warning signals to failure have been identified, even in the AE analysis. In situ any precursory signals are most likely to be from with AE signatures, in particular their location, frequency character, the ratio of the cumulative hits and the cumulative energy parameter detected with AE sensors local to high risk fracture zones. Such data might allow the assessment of what stage/type of failure is occurring and so the state of coalescence of the fracturing might be inferred. Even though the observations showed that the coalescence mechanisms may lead very rapidly to failure with only a slight prior warning from the AE monitoring, in situ collapses will occur as the result of many such rock-bridge failures and under different stress conditions. Therefore monitoring with AE within the cavities below Naples may allow tracking of rock-bridge failures and assessment of the overall likelihood of block detachment and large failures. In this research, the effect of non-persistent joint on the shear behavior of rock bridge is ambiguous

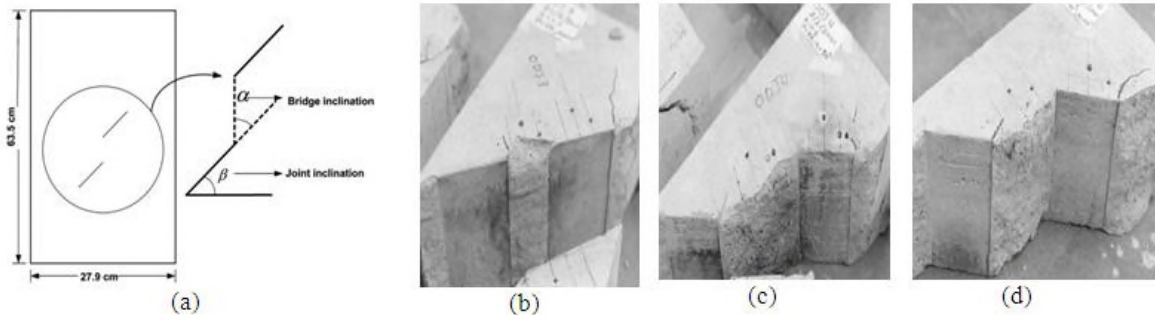


Fig. 3 (a) Geometry of specimens and the pre-existing cracks, (b) Upper side of the failure surface  $K = 0.6$ ,  $\alpha = 0^\circ$ ,  $\beta = 45^\circ$ , (c)  $K = 0.6$ ,  $\alpha = 30^\circ$ ,  $\beta = 45^\circ$ , (d)  $K = 0.6$ ,  $\alpha = 45^\circ$ ,  $\beta = 45^\circ$ , Mughieda *et al.* (2004)

Mughieda *et al.* (2004) has investigated the Fracture mechanisms of offset rock joints under uniaxial loading (Fig. 3). The inclination angle of the joints ( $\beta$ ) remained constant at  $45^\circ$  for all specimens and the inclination angle of the bridge ( $\alpha$ ) was changed from  $0^\circ$ - $120^\circ$  with an increment of  $15^\circ$ . The ratio of rock bridge surface to total shear surface was 0.6 ( $K=0.6$ ).

In all specimens, the wing cracks were initiated and propagated before the failure, due to high concentration of tensile stresses at the joint tips. Mode of failure was dependent on the crack-bridge configuration (Fig. 3(b), (c) and (d)). Bridge inclination was the main variable that controlled the mode of failure. For bridge inclination of  $30^\circ$ ,  $45^\circ$ ,  $90^\circ$ , and  $105^\circ$ , the coalescence occurred due to mixed tensile and shearing failures. For bridge inclination of  $60^\circ$ ,  $75^\circ$  and  $120^\circ$ , coalescence was due to pure tensile failure. For non-overlapped joints, the strength of specimens was the highest for coplanar joints and the lowest for bridge inclination angle of  $30^\circ$ . Mixed mode of failure controlled the strength of offset joints. For overlapped joints, the strength increased as the bridge inclination angle increased. Difference in displacement between the bridge and the joint proves that there was progressive failure. In this research, the effect of confining pressure on the shear behavior of rock bridge are ambiguous. Also, the effect of joint persistency on the failure pattern has been eliminated.

Mughieda *et al.* (2006) has investigated the Coalescence of offset rock joints under biaxial loading (Fig. 4). Inclination angle of the joints ( $\beta$ ) remained constant at  $45^\circ$  for all specimens and inclination angle of the bridge ( $\alpha$ ) was changed from  $0$  to  $90^\circ$  with an increment of  $15$ . The specimens were tested under three different confining stresses: 0.35, 0.7 and 1.5 MPa, and the lateral stress to unconfined compressive strength (11 MPa is an average value) ratios were: 0.032, 0.064 and 0.14, respectively. Experimental study proved that, the coalescence mechanism and the strength of jointed blocks with open offset rock joints were highly dependent on the bridge inclination angle. In all specimens, wing cracks initiated and propagated before the failure due to high concentration of tensile stresses at the joint tips. For low confining stress, wing cracks appeared in the middle of joints. The mode of failure was dependent on the crack-bridge configuration. Bridge inclination was the main variable that controlled the mode of failure. For bridge inclination of  $0^\circ$ , the coalescence occurred due to shear failure and for bridge inclination of  $90^\circ$ , the coalescence occurred due to tensile failure while for the other bridge inclinations, coalescence occurred due to mixed tensile and shear failure. Results showed that for non-overlapped joints, the strength of specimens was the highest for coplanar joints and the lowest for bridge inclination angle of  $30^\circ$ . Mixed mode of failure controlled the strength of offset joints. In

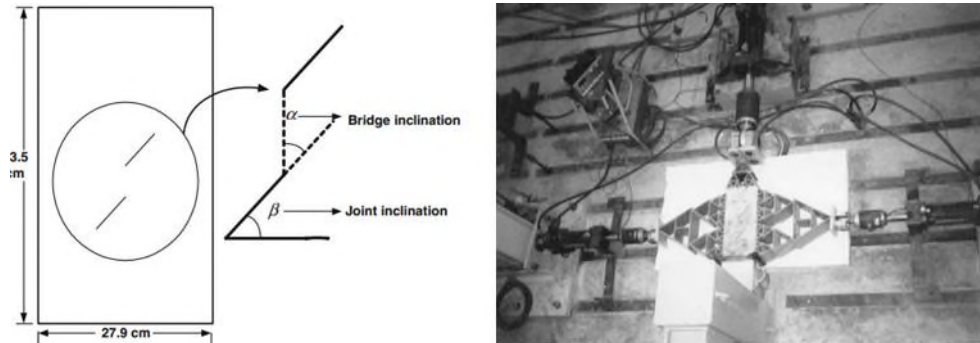


Fig. 4 Geometry of specimens and the pre-existing cracks, b) Biaxial testing equipment, general set-up, Mughieda *et al.* (2006)

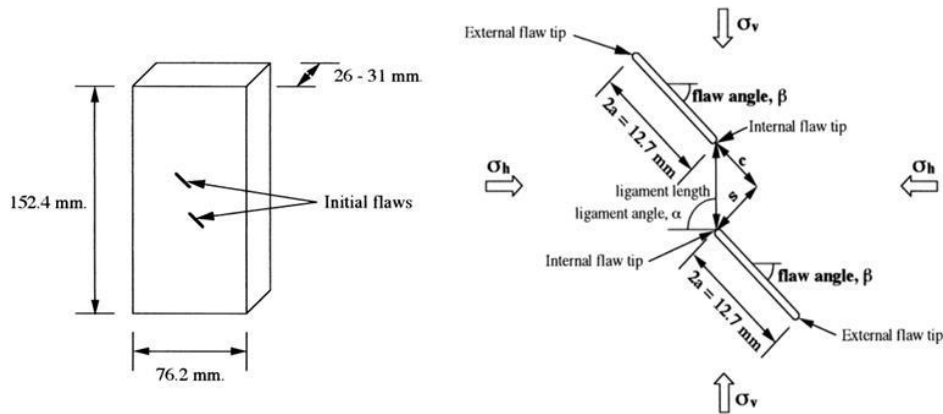


Fig. 5 Geometries of model rock specimen. a) Overall view, (b) detail, Bobet and Einstein (1998)

this research, the effect of confining pressure has been investigated only in two direction. Also, the effect of joint persistency on the failure pattern has been eliminated. In this research dimension of sample is small and scale effect was absent in the research.

Bobet and Einstein (1998) have been investigated the fracturing coalescence in rock type material under uniaxial and biaxial compression (Fig. 5). the flaw angles ( $\beta$ ) were set at  $30^\circ$ ,  $45^\circ$  and  $60^\circ$ , the spacing ( $s$ ) was 0 to  $4a$  and the continuity ( $c$ ) was from  $a$  to  $4a$ . The flaw types were either open or closed.

Results showed that by increasing confining stresses, wing cracks initiations which were expected to occur at flaw tips shifted towards middles of the flaws. Secondary cracks which in some cases were actually appeared before the wing cracks, involved in cracking coalescence. Both types of cracks grow stably to a point before the coalescence, when unstable propagation of secondary cracks takes place. A very interesting observation relates to the influence of ligament length is, i.e. distance between the flaws. Up to a distance of 1.5 times of the flaw length, flaws effect on each other during the crack growth; also coalescence can only occur if flaws are sufficiently close to each other, a distance which decrease with increasing confining stress. It is also significant to mention that, the secondary cracks initially propagate in shear in many cases up to the coalescence. In this research, the effect of confining pressure has been investigated only in two directions. Also, the effect of joint persistency on the failure pattern has been eliminated. In

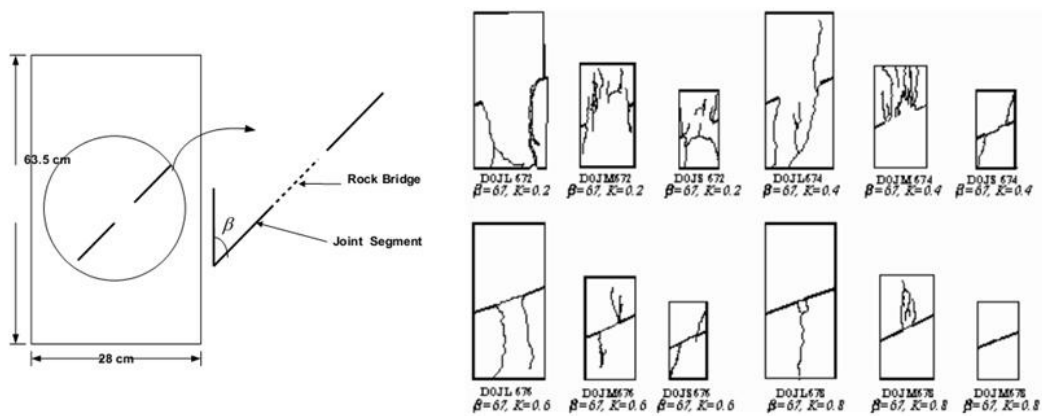


Fig. 6 Scale effect on the mode of failure,  $\beta = 67^\circ$ , Mughieda *et al.* (2004)

this research dimension of sample is small and scale effect was absent in the research. It's to be note that the spacing and continuity of rock joint have important effect on the failure behaviour but this effect has been eliminated due to small scale of sample.

Mughieda *et al.* (2004) has investigated the scale effect on engineering properties of open non-persistent rock joints under uniaxial loading (Fig. 6). Uniaxial compression tests were performed on blocks made of rock like material. Three block sizes were tested having dimensions of  $(63.5 \times 28 \times 20.3)$  cm,  $(40.7 \times 20.3 \times 13.5)$  cm and  $(30.5 \times 15.24 \times 10)$  cm with different degrees of persistence (K) (joint length percentage of the total non-persistent length; 0.2, 0.4, 0.6 and 0.8) and joint angle. Joint angles ( $\beta$ ) were set at  $45^\circ$  or  $67.5^\circ$

Results showed that there are two modes of failure; shearing failure along the non-persistent joints, and the failure through intact materials, depending upon the following three factors: As  $\beta$  increases, mode of failure changes from failure through intact material to shearing along the non-persistent joints. As K increases, the mode of failure tends to change from splitting failure in intact materials to shear failure along the planes of non-persistent joints. As sample size decreases, the mode of failure changes from splitting failure in intact materials to shearing failure along the planes of non-persistent joints. As size increases, strength decreases. In this research, the effect of confining pressure on the shear behaviour of rock bridge is ambiguous. Also, the effect of number of joints on the failure pattern has been eliminated

Since in rock masses, a number of discontinuities are present, the question remains as whether the observations from specimens with two flaws can be extrapolated to specimens with multiple flaws. Lin *et al.* (2000) and Wong *et al.* (2000) reported very briefly the results from specimens containing multiple flaws under both uniaxial and biaxial compression. Number of flaws in specimens was from 3 to 42. To study the failure of brittle rocks consisting non-persistent joints, Nemat-Nasser and Horii (1982), Horii and Nemat-Nasser (1985, 1986) investigated the mechanism of crack interactions and the final failure patterns in fractured (flawed) plates made of Columbia resin CR39 under uniaxial, as well as biaxial compressions. Their specimens contain a series of flaws of different lengths and orientations (Horii *et al.* 1985). They showed that the flaw length is one of the parameters controlling failure patterns specimens. In general, larger flaws control mechanism of coalescence in the form of axial splitting under uniaxial compression with little or no crack growth from small flaws. Under biaxial compression, the growth of larger flaws is followed by the growth of smaller flaws and the final failure is a coalescence of smaller flaws in

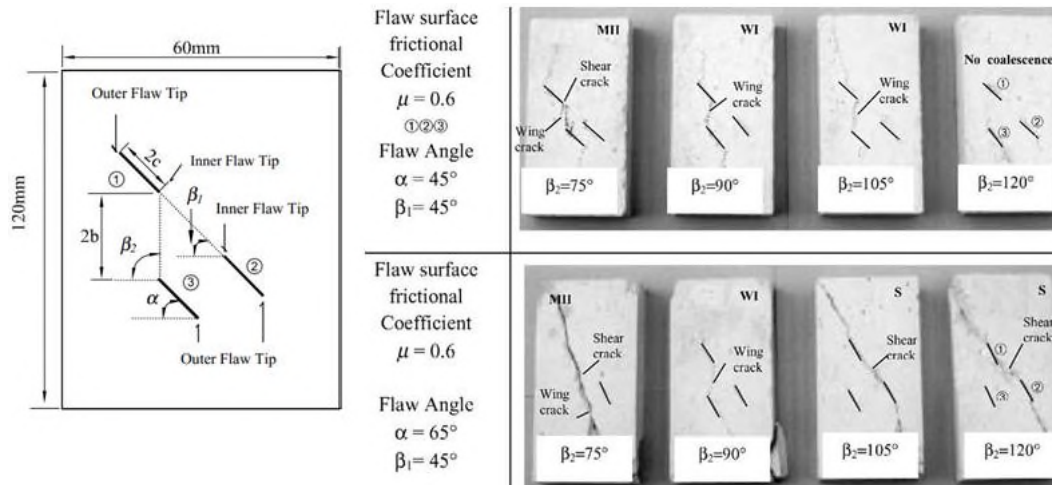


Fig. 7 The specimen containing three flaws, Wong *et al.* (2001)

a form of shear zone or fault.

Wong *et al.* (2001) investigated the crack coalescence in rock-like materials containing three flaws (Fig. 7). The inclinations of the pre-existing flaws used in this study were  $45^\circ$  and  $65^\circ$ . The bridge angle of  $b$  was fixed at  $45^\circ$ , while  $b$  varied from  $75^\circ$  to  $120^\circ$ . Length of flaw  $2c$  was fixed at 12mm. Bridge distance between the two flaws  $2b$  was fixed at 20 mm.

Results show that the crack coalescence occurs between only two flaws (not three). The mechanisms of crack coalescence depend on coalescence stress of the pair of flaws. The lower value of coalescence stress between the pair of flaws will dominate the process of coalescence. Mixed and wing tensile modes of coalescence are more likely to occur in respect to the shear mode, if coalescence stress between a pair of flaws be very close to (within 5% of each other). Frictional coefficient  $m$  of flaw surface can affect the pattern of coalescence of cracked solids. Uniaxial peak strength for cracked specimens does not depend on the total number of flaws but only on the number of flaws which actually involved in forming shear zone of failure pattern. In this research, the effect of confining pressure on the shear behaviour of rock bridge is ambiguous. Also, the effect of number of joints on the failure pattern has been eliminated. It's to be note that the behaviour of sample consisting rock joint with various direction is ambiguous.

Kuntz *et al.* (1998) has used the steady-state flow experiments to visualise the stress field and potential crack trajectories in a 2D elastic-brittle cracked media for uniaxial compression. Several experiments with one single, two en-echelon and randomly distributed cracks have been conducted and compared with analogue data in two-dimensional elastic plates. It is shown that the steady state flow method not only provides an accurate picture of crack-induced perturbation of the displacement field but may also be used to predict the potential trajectories of mode I cracks. Micro mechanisms of the cracks interactions such as screening or enhancing effects are well illustrated. Since the coalescence is observed only for few favourable initial configurations of pre-existing flaws, the emergence of a macroscopic failure still remains an open question.

Sagong *et al.* (2002) have been conducted a number of experiments on pre-cracked specimens, made of gypsum loaded in compression (Fig. 8). Two series of tests have been investigated: specimens with three flaws, and with 16 flaws. The objective of their research is to ascertain if the

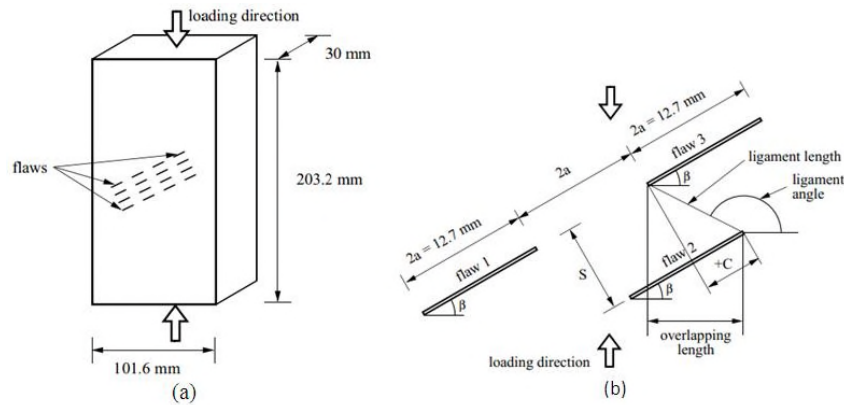


Fig. 8 Specimen with multiple flaws, (a) Overall view, (b) geometry of the flaws, Sagong *et al.* (2002)

crack types and coalescence patterns produced in specimens with two flaws can be extrapolated to specimens with three and 16 flaws. Three parameters are changed to produce different geometries (Fig. 8(b)): flaw inclination angle,  $\beta$ ; spacing,  $S$ ; and continuity,  $C$ : All flaws were parallel to each other and have the same angle  $\beta$  with the Horizontal (i.e. the horizontal is defined as perpendicular to the direction of loading). Three flaw inclination angles were at:  $30^\circ$ ,  $45^\circ$ , and  $60^\circ$ . Spacing,  $S$ ; is the distance between the two contiguous rows of flaws, and is measured along a direction perpendicular to the planes of the flaws. Two different spacing are used;  $a$ , and  $2a$  (i.e. 6.35 and 12.7mm);  $2a$  refers to the length of flaw, and  $a$ , half-length of flaw; all flaws had the same length,  $2a = 12.7\text{mm}$ ). Continuity,  $C$ ; is the distance between the flaws in two different rows, and is defined as the overlapping length between two flaws measured along the planes of the flaws (see Fig. 8(b)). Continuity can be positive (as in Fig. 8(b)), or negative (for example, if the right tip of flaw 2 (one side of the crack) in the figure is between flaw 1 and flaw 3). Five investigated continuities were:  $-2a$ ,  $-a$ ,  $0$ ,  $a$ , and  $2a$  (i.e.  $-12.7$ ,  $-6.35$ ,  $0$ ,  $6.35$  and  $12.7\text{mm}$ ). Distance between flaws on the same row was kept constant for all tests and equal to  $2a$  (12.7mm; see Fig. 8(b)).

Results showed that the initiation stresses for wing crack and secondary crack were dependent on the geometry of flaws. Initiation stress increases with; the flaw angle, the spacing, the overlapping ratio, and decreases with the number of flaws.

Coalescence was produced by the linkage of two flaws through wing and/or secondary cracks. Linkage can be produced by any combinations of wing cracks and secondary cracks. Nine types of coalescence have been identified based on the nature of the cracks involved. Type of coalescence can be correlated with the geometry of flaws, defined by the flaw inclination angle and the ligament angle. Coalescence Type I occurs in coplanar flaws; coalescence Type II in non-overlapping left stepping flaws; coalescence Type IV in overlapping left stepping flaws; coalescence Type III is a transition between Types II and IV (i.e. transition between non-overlapping and overlapping); coalescence Type V for perfectly overlapping geometries; coalescence Type VI for overlapping right stepping geometries; coalescence Types VIII and IX for non-overlapping right stepping geometries; coalescence Type VII is a transition between Types VI and VIII (i.e. between overlapping and non-overlapping). Coalescence stress increases with flaw inclination angle and ligament length. For ligament lengths greater than  $3a$ , the joint length would be  $2a$  and the coalescence stress stays constant and it is rather independent of the relative locations of flaws. Coalescence in specimens with multiple flaws tends to occur in a ‘‘columnar’’ pattern

where flaws in the same column are linked together. The right and left stepping failures observed in three flaws samples occurred for the samples consisting 16 flaws too. In this research, the effect of confining pressure on the shear behavior of rock bridge is ambiguous. Also, the behavior of sample consisting rock joint with different direction is unknown. It's to be note that the result of this research was restricted to gypsum. It's important to clarify what is the behavior of rock bridge when inserted in different materials.

Prudencio *et al.* (2007) has investigated the strength and the failure modes of rock mass models with non-persistent joints (Fig. 9). Joint geometries and confining stresses are shown in Table 1. Results show that, stress orientation relative to joint orientation and the value of confining stress are concluded from different failure modes. Samples with steeply dipping non-persistent joints and the joint step angles larger than 90° underwent planar failure. Strengths of some samples turned out to be larger than those predicted by a simple model, because normal stress on rock bridges is several times larger than that assumed by simple (intact) model. Low confining pressures when the joint step angle is approximately 90° can induce a step failure along an average slope angle of  $\psi_f = \psi_1 + \Delta\psi$ , where  $\psi_1$  is the dip of joint system and  $\Delta\psi = \tan^{-1}(d/L_j)$  ( $d$  is the joint spacing and  $L_j$  is the joint length). Wing fractures and tensile failure propagating in the rock bridge between the parallel adjacent fractures can significantly reduce the strength of rock mass. As a result, the model divides into a series of individual blocks which can rotate, leading to a toppling or “rotational failure”. The overall strength can be as low as the residual strength on an equivalent joint along

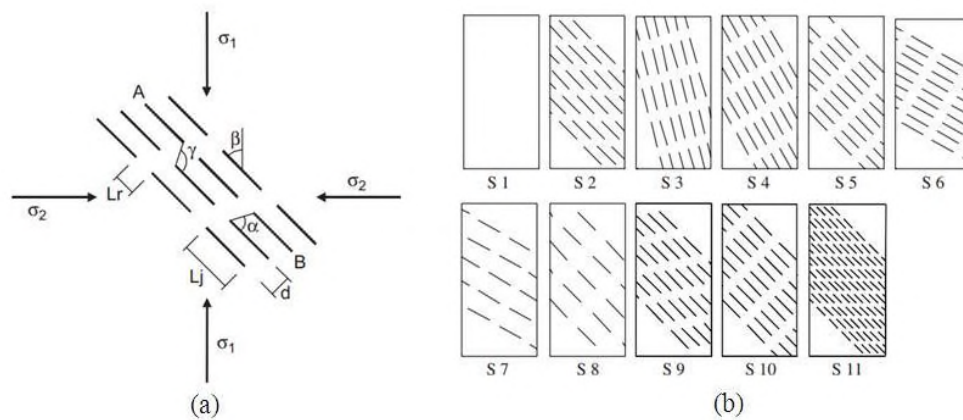


Fig. 9 (a) Parameters varied in the tests, (b) Joint geometries tested, Prudencio *et al.* (2007)

Table 1 Joint geometries and confining stresses of the samples tested, Prudencio *et al.* (2007)

Serie	$L_j$ (cm)	$L_r$ (cm)	$d$ (cm)	$\gamma^\circ$	$\beta^\circ$	$e$ (cm)	$\sigma_2/\sigma_c$
1	5	2	2	—	—	0.01	0.000 0.050 0.169
2				90	45		0.000 0.026 0.040 0.050 0.096
3				135	15		0.000 0.043 0.047 0.103 0.169
4					30		0.000 0.017 0.023 0.053 0.091 0.103 0.169
5					45		0.000 0.040 0.064 0.126
6					60		0.000 0.011 0.025 0.035 0.060 0.077 0.079 0.176 0.199
7			4	117			0.000
8		3		127	45		0.000 0.011 0.020 0.039 0.058 0.086
9		2	2	112.5			0.000 0.030 0.055 0.075 0.100
10				135		0.00	0.000 0.042 0.066 0.123
11	2.5	1	1	90		0.01	0.000 0.099

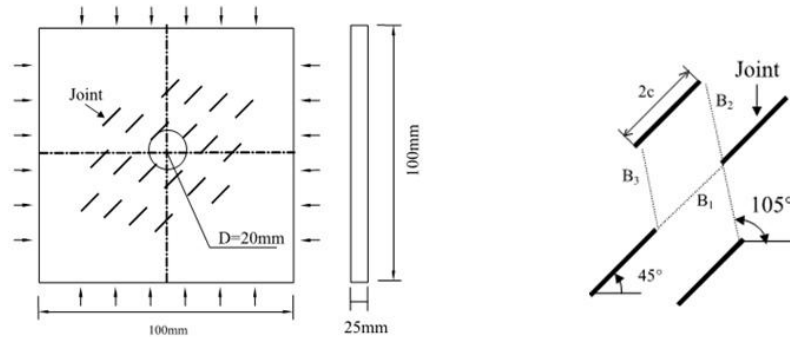


Fig. 10 Geometry of model rock-like specimen. B1, B2 and B3 are the distance between two joints, Wong *et al.* (2002)

the potential failure surface. Planar failure and stepped failure are associated with higher strengths, brittle behaviour, and small failure strains, while rotational failure is usually associated with a very low strength, ductile behaviour, and large deformation. The ability to forecast failure mode has a significant economic effect on open pits stabilities: rotational failure would lead to a regressive slope failure, while a planar failure, although associated with a possible steeper pit, would lead to a brittle behaviour of the slope.

In this research, the effect of confining pressure has been investigated only in two directions. Also, the effect of joint persistency on the failure pattern has been eliminated due to restrict in sample dimension. In this research sample is small. Scale effect was absent in the research. Wong *et al.* (2002) has investigated creeping damage around an opening in rock-like material containing non-persistent joints (Fig. 10). The locations and orientations of slots are pre-determined by giving a fixed arrangement of joints. The lengths ( $2c$ ) and the angles of joints are fixed at 10 mm and at  $45^\circ$ , respectively. Lengths of the three bridges (the distance between the two joints, i.e. B1, B2, B3) are fixed at 10 mm. For all specimens, the angle of bridge  $\beta_2$  or  $\beta_3$  is fixed at  $105^\circ$  while the bridge angle for  $\beta_1$  at  $45^\circ$ . Two types of stress levels are applied on the jointed specimen with an opening, to study the creeping damage after excavation. For the first type stress level, the  $\sigma_3$  value is changed with a fixed stress of  $\sigma_1$ . The fixed  $\sigma_1$  is set at 1.2 MPa, at 65% of  $\sigma_{1max}$ . This fixed  $\sigma_1$  (1.2 MPa) is the average stress level required to cause crack initiation in jointed specimen. The  $\sigma_3$  changes is varied from  $\lambda$  ( $\sigma_3/\sigma_1$ ) = 1/3 to 1 with 1/6 increment. Second type of stress level is based on the changes of  $\sigma_1$  with a fixed  $\lambda$  value. The  $\sigma_1$  is changed from 45% to 85% of  $\sigma_{1max}$  with 20% increment. Thus, applied  $\sigma_1$  are changed from 0.8, 1.2 to 1.6 MPa. These three stress levels represent the stress below, at, and above the crack initiation stress. With a fixed  $\lambda$ , the applied  $\sigma_3$  will also be varied with the changes in  $\sigma_1$ . For a systemic studying on creeping around the excavated opening, the  $\lambda$  value is also varied from 1/3 to 1. With these variations, the effects of in situ stress level on failure mechanisms and the creeping time to failure could have been fully studied.

Results show that, when the stress ratio  $\lambda$  ( $\sigma_3/\sigma_1$ ) is low (1/3), the tensile mode of creeping failure is dominant and with high stress ratios of ( $\lambda > 1/2$ ), the shear mode or a combined tensile and shear mode are.

For a lower  $\lambda$  ( $\lambda \leq 1/3$ ), the micro-fractures are induced and propagate stably towards the neighbouring joints, opening with a stepwise increasing until final failure. For a higher  $\lambda$  ( $\lambda > 1/2$ ), deformation around the opening fluctuate slightly after the excavation, then sudden failure. For  $\lambda$

$\geq 2/3$ , no deformation changes after the excavation momentarily, then sudden failure. Deformation around the opening decreases distance away from it where the strain of the inner zone ( $r \leq 1.7 a$ ) is about four times larger than that of the strain in the outer zone ( $r > 1.7 a$ ). For a high stress ratio of  $\sigma_1 / \sigma_{1max} > 65\%$  ( $\sigma_{1max}$ : the peak stress of jointed rock-like specimen without opening), large deformation appears after the excavation. As a result, faster collapses of the opening will occur. When  $\sigma_1 / \sigma_{1max} < 45\%$ , only few cracks initiate and propagate after the opening was drilled. As a result, the opening remains stable. creeping failure time decreases with an increase in stress ratio of  $\lambda$  and  $\sigma_1 / \sigma_{1max}$ . Stress ratios  $\lambda$  and  $\sigma_1 / \sigma_{1max}$  are important indices indicating the degree of instability of an opening after excavation. In this research, the effect of confining pressure has been investigated only in two directions. Also, the effect of joint persistency on the failure pattern has been eliminated due to restrict in sample dimension. In this research sample is small. Scale effect was absent in the research. The effect of tunnel diameter on failure behaviour is unknown. In this research the effect of porosity, density, material mixture has been eliminated.

Rocky landslides contain a lot of rock bridges, and researches on rock bridge were carried out by experimental methods and simulated by analytical and numerical simulation techniques. The laboratory study of AE characteristics during rock stress-strain process was reviewed (Rudajev *et al.* 2000, Jansen *et al.* 1993); real-time failure process (Wang *et al.* 2013) and stability evaluation and harm degree of landslides (Cheon 2011) were marked out. Behavior of rock bridge was observed firstly by shear test in 1990 (Li *et al.* 1990); then cyclic loading test of rock bridge and mechanical behavior was carried out (Shen 1990). The failure mechanisms and pattern of coalescence of rock bridges were investigated (Wong 1999). Strength, deformability, failure behavior, and AE locations of red sandstone were tested by using triaxial compression (Yang, 2012). Analytical methods such as neural network (Ghazvinian 2010), slice element method (Zhang, 2008), and time-dependent degradation failure (Kemeny 2005, Zhu *et al.* 2004) are used to study the progressive failure of rock bridge.

Rocky landslides contain a lot of rock bridges, and researches on rock bridge were carried out by experimental methods. The laboratory study of AE characteristics during rock stress-strain

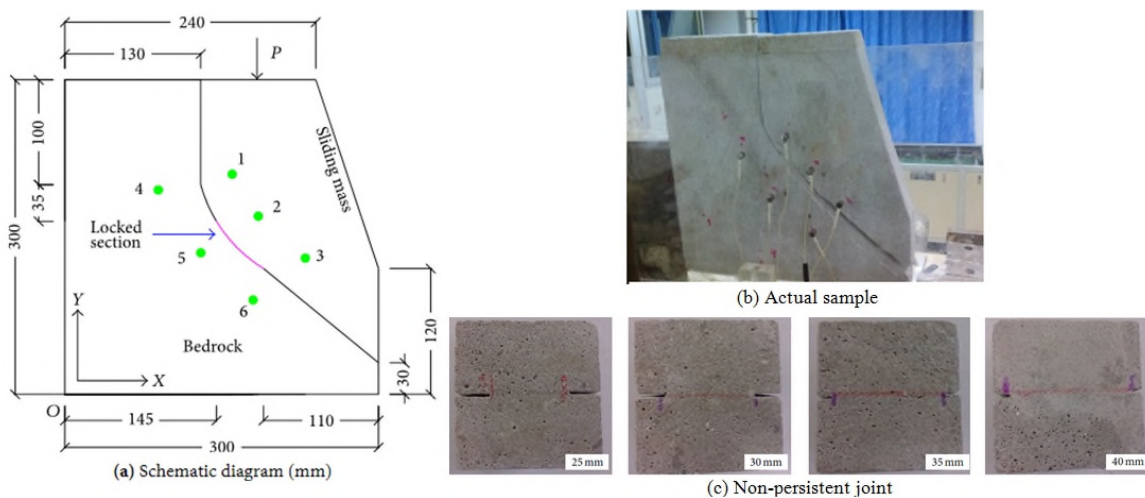


Fig. 11 (a) Sample size and sensor position, (b) Failure of locked section under continuous loading, (c) Different reserved rock bridge length, Chen *et al.* (2015)

process was reviewed (Rudajev *et al.* 2000, Jansen *et al.* 1993); real-time failure process (Wang *et al.* 2013) and stability evaluation and harm degree of landslides (Cheon 2011) were marked out. Behaviour of rock bridge was observed firstly by shear test in 1990 (Li *et al.* 1990); then cyclic loading test of rock bridge and mechanical behaviour was carried out (Shen 1990). The failure mechanisms and pattern of coalescence of rock bridges were investigated (Wong 1999). Strength, deformability, failure behaviour, and AE locations of red sandstone were tested by using triaxial compression (Yang, 2012). Analytical methods such as neural network (Ghazvinian 2010), slice element method (Zhang, 2008), and time-dependent degradation failure (Kemeny 2005, Zhu *et al.* 2004) are used to study the progressive failure of rock bridge.

Chen *et al.* 2015 was investigated the failure mechanism of Rock Bridge based on acoustic emission technique under direct shear test (Fig. 11).

The results show that AE source location can be accurately located during small scale tests in small scale direct shear tests. The AE event count peak value increases with the increasing of rock bridge length and vertical stress. In addition, the time of AE event count peak value appearing goes back with the increase of the length and the vertical stress. AE resource location was accurately and reliably located during large scale landslide model test with locked section. Based on the locating process, rock sample failure features and cracks time-space evolution process were revealed. AE showed that the brittle failure feature of landslide with locked section was reflected well. In this research the effect of echelon joint, joint roughness, joint filling and joint aperture on the failure behavior has been eliminated. Also the effect of material mixture on the failure pattern is ambiguous.

However, most of the previous studies are focused on the mechanisms of crack initiation, propagation and interaction under uniaxial and biaxial compression, but relatively few experimental investigations were done to examine the pattern of crack coalescence in the rock bridge area under direct shear loading. Lajtai (1969a,b) performed direct shear testing on model material with non-persistent joints and observed that, the failure mode changes with increasing normal stress. He suggested a composite failure envelope to describe the transition from tensile strength of an intact material to residual strength of discontinuities. He thus recognized that the maximum shear strength develops only if strength of solid material and the joints are mobilized simultaneously. Savilahti *et al.* (1990) did some further study on the specimens with jointed rock under direct shear testing where the joint separation varies in both horizontal and vertical directions and joint arrangement changes from non-overlapping to overlapping using modelling

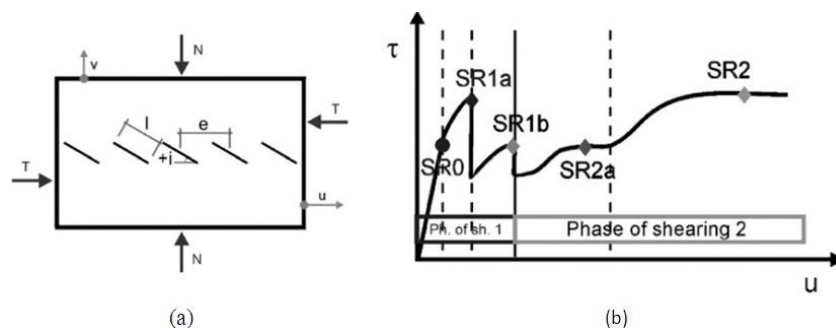


Fig. 12 shear specimen with discontinuous joint. Definition of the geometrical parameters, (b) beginning of idealized shear test record. Shear stress  $\tau$  is shown to vary systematically with growing shear displacement  $u$ , Gehle (2003)

material. The coalescence patterns for specimens indicated that, the jointed rock failed in mixed and tensile modes for non-overlapping and overlapping joint configurations, respectively. Wong *et al.* (2001) studied shear strength and failure pattern of rock-like models containing arrayed of open joints in both modelling plaster material and natural rocks under direct shear tests. Results showed that failure pattern was mainly controlled by the joint separation while shear strength of jointed rock depended mostly on the failure pattern. Ghazvinian *et al.* (2007) made a thorough analysis of the shear behaviour of the rock-bridges based on changes in the persistency of their area. The analysis proved that, the failure mode and mechanism were under continuity effect for rock-bridge. Gehle (2003) investigated breakage and shear behaviour of intermittent rock joints (Fig. 12).

The effect of crack angle  $i$ ; scale and degree of separation ( $l = e$ ; with crack length  $l$  and crack distance  $e$ ) (see Fig. 12(a)), the influence of different crack types and conditions, the influence of normal loading as well as of the kind of loading (CNL versus CNS), and finally, the influence of different model materials on shear failure behaviour of rock bridges has been investigated. These tests revealed that shearing of such joints is characterized by several mechanisms, each responsible for a special kind of shear resistance. Three phases for shearing can be identified. The characteristic or maximum shear resistances in these phases are called SR1 to SR3 (Fig. 12(b)). First shearing phase is that of actual rupture, initiated by the formation of wing cracks (at SR1a), starting from existing cracks and growing into the material bridges, and concluded by generating additional new fractures connecting the initial cracks in the zone between the wing cracks (at SR1b). Complete bisecting of the material bridges is then obtained. The second phase of shearing is characterized by friction processes and volume increase in shear zone. Depending on whether or not the initial cracks are open, the shear resistances representing the levels in the shear curves are called SR2a or SR2. Finally, the third phase of shearing, reached after large shear displacements, is determined by the sliding processes inside strongly fractured shear zone. Here SR3 is the measured resistance.

These shear resistances corresponding to different shear mechanisms depend on various ways of testing conditions. Each can be a maximum shear resistance, so none of the shear mechanisms may be neglected. Of all investigated parameters, the inclination of cracks inside discontinuous joint and the normal stress are found to have dominant effects on shear strength. Their influence varies from phase to phase due to different shear mechanisms. Each shear mechanism has been investigated in detail. Failure of the rock bridges by wing and connecting cracks are shown to be a tensile one. Frictional resistance after the completion of initially discontinuous joint is not only caused by sliding, but by rotation and further breakage as well. The final shear process is characterized by sliding within the rock breccia, into which the rock has been transformed by intensive cracking and crushing. Most important conclusion from the presented results is the fact that, not only one but several shear mechanisms are responsible for the shear strength of a discontinuous joint. Most previous models suggested that, evaluation of the shear strength of discontinuous rocks are usually based on one shear mechanism only or entirely empirical and are therefore not suited for the representation of complete shear process. In this research the effect of joints persistency, joint number, scale effect, material mixture, and echelon joint has been eliminated on the failure mechanism of non-persistent joint. Also the effect of normal load, loading rate, cyclic and dynamic loading are ambiguous on the shear behaviour of non-persistent joint.

Ghazvinian *et al.* (2011) has investigated the effect of joint overlapping on shear behaviour of rock bridge. Four specimens with similar Ligament length of 45 mm and different ligament angles of  $0^\circ$ ,  $25^\circ$ ,  $90^\circ$  and  $115^\circ$  were prepared (Ligament length is the distance between the tips of two

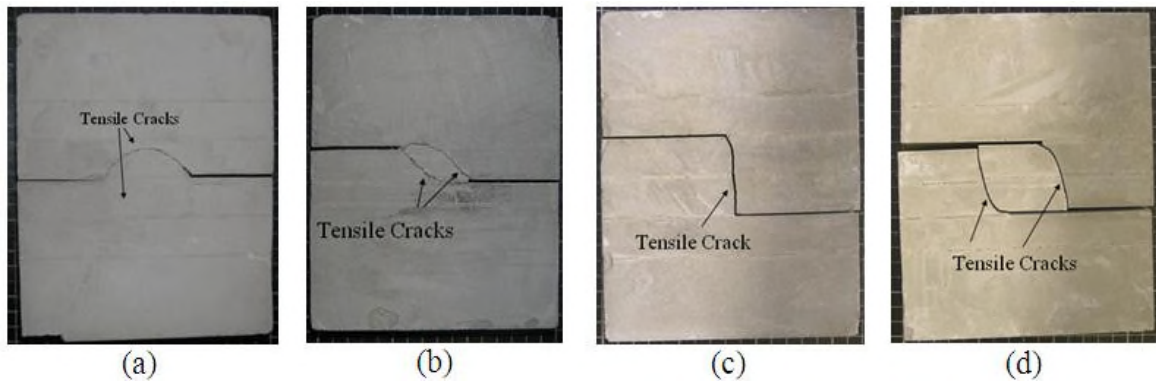


Fig. 13 the crack patterns for ligament angle of; (a)  $0^\circ$ , (b)  $25^\circ$ , (c)  $90^\circ$  and (d)  $115^\circ$ , Ghazvinian *et al.* (2011)

joints and ligament angle is the counter-clockwise angle between the ligament length and shear axis. For different specimens, the lengths of edge joints were different but in same specimen, the lengths of those two joints were similar. The joint lengths (b) were at 52.5, 66.8, 75 and 78.8 mm, associated with the ligament angles of  $0^\circ$ ,  $25^\circ$ ,  $90^\circ$  and  $115^\circ$ ; respectively.

All samples were tested by applying a shear displacement rate of 0.01mm/s. Normal stress applied to the samples was set at 0.1 MPa. Observations showed that ligament angles influence failure pattern of the rock bridge. Fig. 13 shows four different types of failure pattern obtained in direct shear tests. When ligament angle is  $0^\circ$  (Fig. 13(a)), the upper tensile crack propagates through the intact portion area but the lower tensile crack develops for a short distance, and then becomes stable so as not to coalesce with the tip of other joint. When ligament angle is  $25^\circ$  (Fig. 13(b)), the wing cracks initiate at the tip of joints and propagate in curvilinear path till coalesce with the tip of other joint. This coalescence left an elliptical core completely separated from the sample. When ligament angle is  $90^\circ$  (Fig. 13(c)), the tensile crack initiates at the joint tip and propagates through the bridged segment. In this configuration, the rock bridge is broken with a single failure surface. When ligament angle is  $115^\circ$  (Fig. 13(d)), the wing cracks initiate at joint walls and develop nearly in vertical direction. These wing cracks propagate through the intact portion area, till coalesce with the opposite joint tips. This coalescence leave a rectangular core of intact material completely separated from the sample. In these failure patterns, surface of failure at bridge area is tensile because no crushed or pulverized materials and no evidence of shear movement were noticed.

The models with ligament angle of  $0^\circ$  and  $25^\circ$  have the non-linear behaviour in force-displacement curve. The non-linearity in force-displacement curve means that, the wing cracks have a stable growth till the peak shear strength is reached. In other word, the wing cracks are suppressed by external normal stress so they have stable growth. When ligament angles are  $90^\circ$  and  $115^\circ$ , the load-displacement curve is completely linear. It means that, the wing cracks grow unstably as soon as they initiate between the joint. Whereas, the effect of normal load is eliminated on the rock bridge due to joint overlapping, therefore the wing cracks grow unstably. Also results showed that, shear loading capacity of non-overlapped joints is more than that of overlapped joints due to normal load appearances on the rock bridge in non-overlapped joint configuration. In this research the effect of joint number, scale effect, material mixture has been eliminated on the failure mechanism of non-persistent joint. Also the effect of loading rate, cyclic and dynamic loading are ambiguous on the shear behavior of non-persistent joint.

### 3. Numerical simulations

Numerical approach proves the necessity of these studies for rocks in investigating the crack propagation and coalescence because of mechanical and geometrical complexity of most problems. In general, many established numerical techniques can be used, i.e., the finite element method (FEM) (Carpinteri *et al.* 1988), the boundary element method (BEM) (Blandford *et al.* 1981, Altiero *et al.* 1982, Aliabadi *et al.* 1993) or the displacement discontinuity method (DDM). In recent decades, numerous theories for predicting stress distribution and crack propagation have been proposed. For most practical purposes, the three fundamental theories commonly employed are (Vasarhelyi *et al.* 2000): maximum tangential stress theory (Erdogan *et al.* 1963), maximum energy release rate theory (Hussain *et al.* 1974), and minimum energy density theory (Sih 1974). Although, any of the above methods can reasonably predict the tensile crack initiation in any samples under both tension and compression, but they have been unsuccessful for the shear crack initiation (Vasarhelyi *et al.* 2000). The Damage Model of Reyes and Einstein (1991) and the F - criterion of Shen and Stephansson (1994) have been specifically developed for crack coalescence through secondary cracking. Both models were successful using uniaxial compression tests but with limited capabilities (Vasarhelyi *et al.* 2000). Recently, Bobet and Einstein proposed a new analytical criterion for both wing and secondary cracks (Bobet *et al.* 1998). This criterion is based on the assumption that crack initiation depends on the local stress state relative to strength of material rather than on stress intensity factor (SIF).

Using DDM, Scavia and Castelli (1996) and Scavia (1999) have conducted some preliminary work through a numerical technique, BEMCOM, to investigate the mechanical behaviour of rock bridges in materials containing two and three crack-like flaws. In their study, a series of numerical analyses was carried out to evaluate the influence of overlapping, so as to identify a critical value of resistance in the rock bridge. Their results show that, direct and induced tensile crack propagation occurs in either, stable or unstable conditions depending on flaw spacing and the applied confining stresses. Vasarhelyi and Bobet (2000) used the Displacement Discontinuity Method, FROCK, to model the crack initiation, propagation and coalescence between the two bridged flaws in gypsum under uniaxial compression. Their work reproduced the types of coalescence observed in the experiments, and predicted an increase in coalescence stresses with ligament length. While a good agreement between numerical and experimental results was found as for the propagation trajectory of tensile and shear cracks in numerical models containing multi-flaws, few numerical models are able to simulate the global response of the loaded specimens containing multi-flaws. Motivated by the observations experimentally conducted by Horii and Nemat-Nasser (1982), uniaxial and biaxial compression on numerical modelling of samples containing a number of large, pre-existing flaws and a row of suitably oriented smaller flaws are simulated by Tang and Kou using RFPA2D code (1998). Numerical results demonstrate that, with confining pressure, the crack growth is stable and stops at some finite crack length; whereas a lateral tensile stress even with a small value will result in an unstable crack growth after a certain crack length was attained. This numerical modelling clearly demonstrated that RFP2D is a validated tool to simulate not only the crack interaction mechanisms but also the global failure behaviour of sample containing pre-existed crack-like flaws.

Mughieda *et al.* (2008) has investigated the stress analysis for rock mass failure with offset joints using finite element analyses. Results show that in two-dimensional finite element model based on linear elastic material, the tensile stress was mainly responsible for wing crack initiation while the shear stress for the secondary crack.

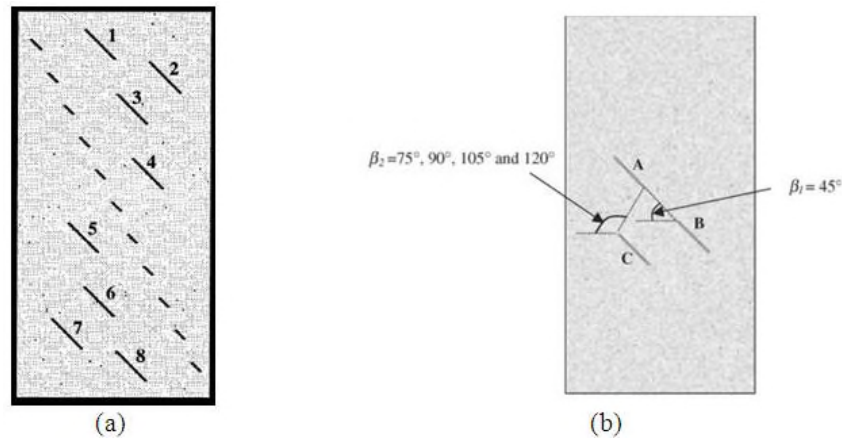


Fig. 14 (a) The numerical model containing a row of small flaws and several larger flaws, Tang *et al.* (1998), (b) Layout of sample containing three pre-existing flaws, Tang *et al.* (2001).

Bremaecker *et al.* (2004) have investigated the shear fracture propagation using displacement discontinuity method (DDM). In this study, one or two cracks were stressed under either uniaxial or biaxial compressions. Two failure criteria have been used; maximum strain energy criterion  $G_{Max}$  and maximum tangential displacement discontinuity,  $D_{sMax}$ .

Results show that in agreement with many previous investigations (Shen *et al.* 1998), under uniaxial stress, propagation occurs by an open wing crack which tends to be in the direction of maximum compressive stress.

Under low lateral normal stress, fracture propagation starts by an open wing crack and continues by a succession of short open and closed segments in a stair step pattern. These segments correspond respectively to wing cracks and shear cracks. It is only in this case that the results of two different propagation criteria for closed cracks,  $G_{Max}$  and  $D_{sMax}$ , differ: both criteria give the same propagation direction for the open segments, but the closed segments are oriented symmetrically with respect to this direction. Numerical considerations suggest that the  $D_{sMax}$  criterion is preferable. As the lateral normal stress increases, the lengths of shear cracks increase at the expense of wing cracks, causing a change in global orientation of the extension. At sufficiently high lateral normal stress, propagation occurs by a purely closed shear crack. These findings confirm Cherepanov's conclusions (1966), which were reached from purely theoretical considerations.

FLAC software has been used to study the effect of two structural planes on the rock strength by Yin *et al.* 2010; Experimental tests and simulation work are conducted by Pu *et al.* 2010 to study the uniaxial strength of the rock contains several structural planes.

Tang *et al.* (1998) have been investigated the crack propagation and coalescence in brittle materials under compression using RFPA2D (Fig. 14(a)). The model contains eleven small flaws (8.6 mm for each flaw in length) and eight large flaws (28.8 mm in length for each), with small flaws arranged in a row. Mesh for the model consists of  $240 \times 120 = 28,800$  elements with geometry of  $200 \times 100$  mm in size. An axial compression is applied to the sample with different confining conditions (compression, tension and no confinement).

Numerical simulations show that micro cracks may nucleate at the tips of flaws and grow in the direction of axial loading. However, the presence of slight lateral tension causes out-of-plane,

curved crack growth in an unstable manner when a suitable critical length was attained. In this case, cracks grow almost spontaneously without an increase in axial compression, leading to sample collapsing in the manner of axial splitting. On the other hand, no unstable growth occurs if a lateral confining pressure is applied to the sample. As a matter of fact, the cracks initiated from the flaw tips and their propagations stop after reaching a finite length. It is confirmed that, under axial compression; nucleation, growth, interaction and coalescence of micro cracks are the dominant controlling sources leading to macroscopic failure of rocks. However, the coalescence of wing-cracks may be in either tensile or shear modes, or a combination of both. Numerical results show qualitatively a reasonably good agreement with reported experimental observations for samples with similar flaw arrangements.

Tang *et al.* (2001) has investigated the crack coalescence in rock-like materials containing three Flaws using RFPA2D. Mesh for the model is  $240 \times 120 = 28,800$  elements representing sample geometry of  $120 \times 60$  mm in scale (Fig. 14(b)). The flaw length,  $2c$ , is 12 mm and the bridge length between the tips of flaws,  $2b$ , is 18 mm. The ratio of flaw length to bridge length ( $c/b$ ) is fixed approximately at 0.66 for all samples. The Inclination of flaws is  $45^\circ$ . The bridge angles between Flaw A and Flaw B ( $\beta_1$ ) are fixed at  $45^\circ$  but  $\beta_2$ , the bridge angles between flaws A and C varies from  $75^\circ$  to  $120^\circ$ .

Results show that there are two types of cracks initiated from the flaw tips: wing cracks and secondary cracks. Wing cracks initiate at an angle with the pre-existing flaw and tend to propagate towards the loading direction. Secondary cracks, however, initiate in a direction coplanar or quasi-coplanar to the pre-existing flaw. Four coalescence modes are observed; tensile wing crack linkage, en-echelon tensile crack forming a shear failure band, pure shear, and mixed mode in tensile and shear. Their relative contribution to crack coalescence depends on the geometry of the pre-existing flaws in the sample. Numerical simulations confirm the coalescence rules that have been found in experiments, called the ‘‘weakest coalescence path’’ either in terms of coalescence stress or coalescence mode. Crack coalescence will occur between the flaws for which the coalescence stress is lower; and the tensile or mixed mode crack coalescences dominate over shear modes when the coalescence stresses are similar.

Li *et al.* (2005) has investigated the failure behaviour of pre-cracked models under compression using RFPA2D. Under uniaxial compression, the basic characteristic of crack propagation was that wing cracks and secondary cracks usually initiated from tips of the fractures. This is coincident

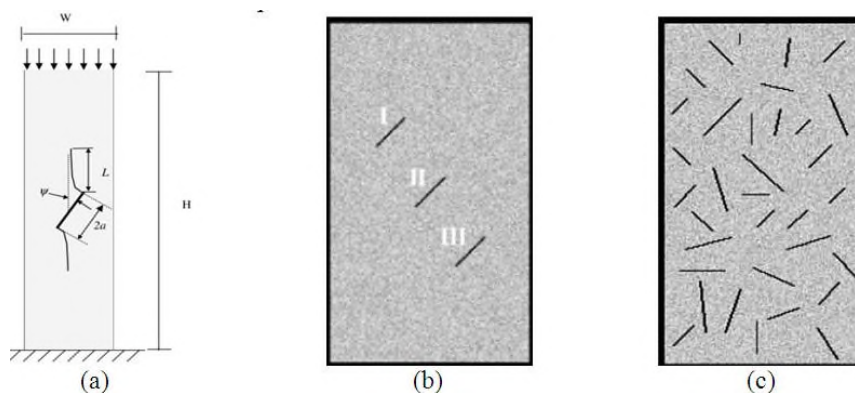


Fig. 15 Schematic of numerical specimen with (a) Pre-existing single flaw, (b) three array flaws and (c) a number of randomly distributed crack-like flaws, Wong *et al.* (2002)

with both of the analytic results of classical fracture mechanics and experimental results.

Wong *et al.* (2002) have investigated the splitting failure in brittle rocks containing pre-existing flaws under uniaxial compression using RFPA2D (Fig. 15). Pre-existing single flaw with the length  $2a$  of 10, 20 and 30 mm is numerically simulated to examine the influence of flaw length on wing crack growth (Fig. 15(a)). Specimens are 50 mm wide, with flaw angle  $w$ , inclining  $45^\circ$  to the axial of compression direction. Numerical specimen is of 170 mm high and 50 mm wide. In order to study the influence of geometric settings on crack-like flaws and the interactions between them, specimens of 170 mm high and 100 mm wide containing three arrays of flaws with the same length  $2a$ , of 20 mm were numerically tested (Fig. 15(b)). Also specimen containing a number of randomly distributed crack-like flaws with different lengths and angles has been modelled (Fig. 15(c)).

Results show that, independent of the specimen size, cracks are easier to nucleate from larger flaws than from the smaller. For the same size (width and length) specimen, growth rate of longer flaw in specimen is generally about twice of which containing shorter flaws. For flaws with orientation of  $60^\circ$  to axial loading direction, crack grows most easily. Wing cracks grow more easily in narrow specimens and split it into columns. For wing cracks approaching to upper and bottom boundaries, growth of the wing cracks slow down. For distance (between the tip of a flaw and free boundary) of less than twice of the flaw length, shear failure may occur, if the shear stress around the flaw tips becomes high enough. For distance smaller than the half-length of flaw, strong interaction between the cracks and the free boundary occurs, causing buckling type failure. Length and location of flaws are important factors to determine the crack nucleation. In general, longer flaws and being closer to specimen free boundary makes the crack nucleation easier. Stress interaction is the most important factor affecting the initiation and propagation of crack from the tips of flaws. For flaws arranged in a diagonal line on specimens, cracks generally grow more easily; but for vertical or horizontal arranged, the growth of middle flaws will be suppressed by stress interactions from nearby flaws.

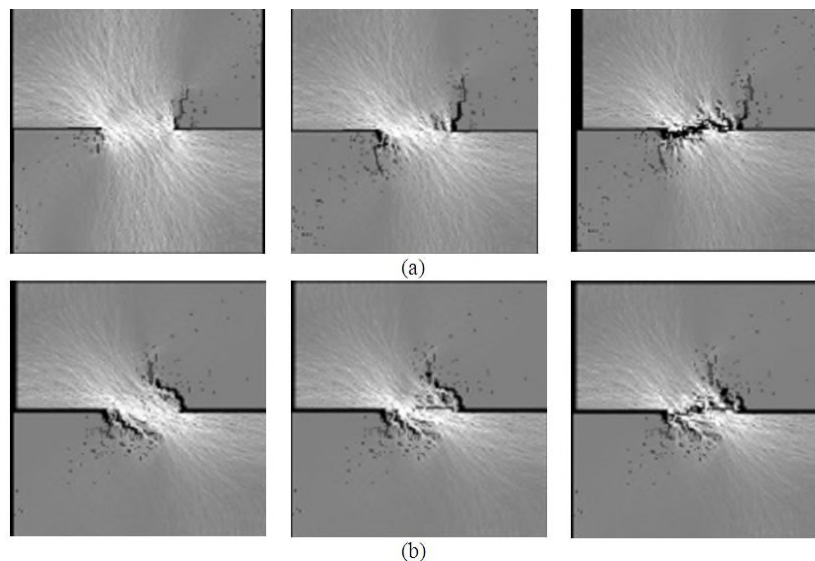


Fig. 16 The shear fracture propagation process in the shear-box test under (a) high confinement, (b) low con confinement, Liu *et al.* (2004)

Zhao *et al.* (2013) were analysed the Fracture of Rock Bridge under shear pressure using FLAC3D. The results shows that firstly the shear stress increases with increasing tangential displacement at the stage before rock bridge fracture and then the shear stress decreases as the tangential displacement increases at the fracture developing stage. Thirdly the sliding along the joint planes is caused and the shear stress increases with increasing tangential displacement. Finally, the shear stress decreases as tangential displacement increases and the value decreases to the residual strength of structural planes.

Liu *et al.* (2004) has investigated the shear fracture of non-persistent joint in heterogeneous rock under direct shear test using numerical simulation (Fig. 16). The rock and tool interaction code (R-T2D), which is developed on the basis of rock failure process analysis (RFPA) model (Tang 1997) and the finite element method, is used to simulate the progressive shear fracture process in shear-box test. The model dimension is  $70 \times 70 \text{ cm}^2$ , rock bridge length is 20 cm. Lateral confinements are 15 MPa and 30 MPa.

Results show that under high confined condition, initially; tensile crack is initiated at the notch tip and propagated in a direction perpendicular to loading direction, then the shear crack initiated at the kink tip, left by the notch and the tensile crack propagate towards the centre of ligament, finally the shear cracks initiated from the two notches coalesce with each other. It is found that heterogeneity and confinement have important influences on the formation and characteristics of shear fracturing in a shear-box test. Because of the heterogeneity, there would be failure events even in initial loading stage and also some in between the bridge area during subsequent loading stage. In a shear-box test under low confinement, the fracturing initiation, propagation and coalescence could be caused by the mixed tensile and shear failure. But the dominant mechanism is a tensile failure instead of shear failure, where initially the tensile crack initiated at notch tip and propagates out of the maximum shear stress zone to form a wing crack. Then with the propagation of wing cracks, an elliptical core is formed between the two tips of prefabricated cracks. Finally a tensile crack suddenly appears at the centre of the ligament and quickly propagates to both tips of the notches to cause coalescences. Moreover, calculated mode II of fracture toughness is increased a little bit with the confinement increasing.

Zhang *et al.* (2006) have been investigated the shear behaviour of intermittent rock joints with different geometrical parameters under direct shear test using RFPA2D (Fig. 17). The geometry of model is  $100 \text{ mm} \times 100 \text{ mm}$ . The Edge-notched joint length ( $b$ ) is 10 (mm), Imbedded joint

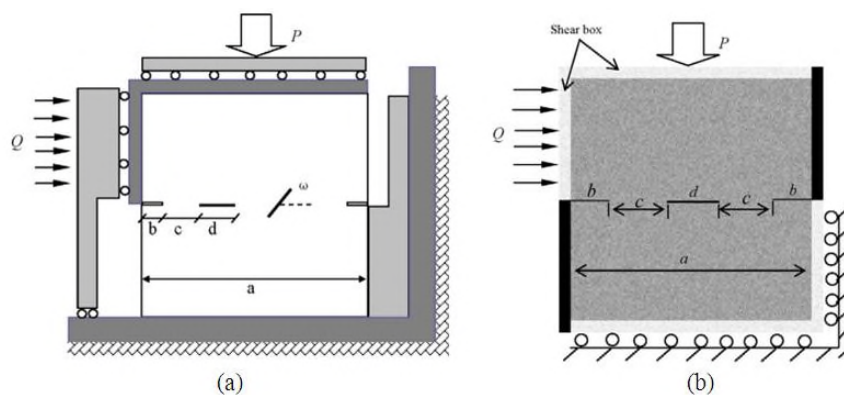


Fig. 17 (a) The sketch map of rock specimen and (b) one example of numerical specimen under direct shear loading condition, Zhang *et al.* (2006)

length ( $d$ ) is 16 (mm), Joint azimuth angle ( $\omega$ ) is  $0^\circ, 15^\circ, 30^\circ, 45^\circ, 60^\circ, 75^\circ, 90^\circ, -15^\circ, -30^\circ, -45^\circ, -60^\circ, -75^\circ$  and Normal stress ( $P$ ), 0.15 (MPa).

Results show that the failure pattern is mostly influenced by geometrical parameters (joint separation and joint azimuth angle), while shear strength is closely related to failure pattern and its mechanism. The following preliminary conclusions can be drawn from numerical tests: Wing cracks normally initiate from the tips of pre-existing imbedded joints with an initiation angle due to strong stress interaction between the joints. Wing cracks propagate towards neighbouring joints through the rock bridge. In the cases of long joint separation, wing cracks will connect each other by newly fractured cracks. Damaging the inner joints by wing cracks formation and coalescence controls further shear processing. It dominates the eventual failure pattern and determines the peak shear load of rock specimen.

Macro shear fracture results from the mesoscopic tensile damage of a large number of elements. The whole fracture process can be divided into three phases: (1) damage of inner configuration; (2) rapid propagation and connection with other cracks; (3) friction process after the total rupturing of bridged rock. The peak shear load is a function of joint angle, and the shear strength has a close relationship with its defect configuration, which is influenced by microscopic defects and macroscopic joints.

Discrete element method (DEM) is also another capable method of studying the failure behaviour of bonded geo-materials (Potyondy and Cundall 2004). Kulatilake *et al.* 2001 established a jointed rock model using adjacent flaws investigating the mechanical behaviour of jointed rock model under uniaxial loading. Zhang *et al.* (2012, 2013) studied crack initiation, propagation and coalescence using one, two or three open flaws. Many types of crack initiation and coalescence observed numerically were similar to the ones observed in laboratory tests. Smooth-joint was found to be a better way to model the mechanical behaviour of a joint in PFC modelling. Bahaaddini *et al.* (2013) used the smooth-joint in a bonded particle model to investigate the effect of joint geometrical parameters on mechanical properties of a non-persistent jointed rock mass under uniaxial compression.

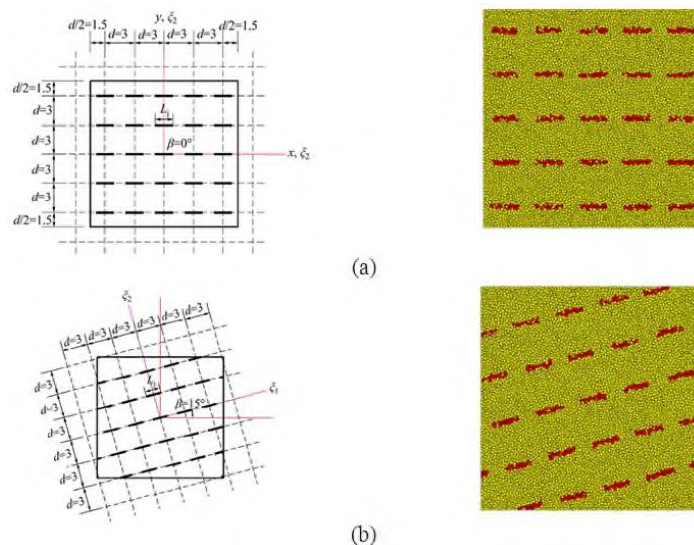


Fig. 18 Joint geometry configurations for a)  $\beta=0^\circ$  and b)  $\beta=15^\circ$ , Xiang *et al.* (2015)

Xiang *et al.* (2015) has investigated the crack initiation stress and strain of jointed rock containing multi-cracks under uniaxial compressive loading using PFC2D (Fig. 18).

The following two parameters are used to design the joint geometry configurations in investigated blocks, the joint inclination angle,  $\beta$ , and the joint continuity factor,  $k$ , (the joint length percentage of the total non-persistent length). The joint configuration for  $\beta=0^\circ$  is shown in Fig. 19(a). The other joint configurations result when the block is rotated contrary to  $z$  axis in counter-clockwise direction for an increment of  $15^\circ$  until the inclination angle reaches  $90^\circ$  (Fig. 19b). When the  $L_j$  (length of a single joint) gets the values of 6, 12, 18 and 24 mm;  $k$  takes 0.2, 0.4, 0.6 and 0.8, respectively. When  $\beta=15^\circ, 30^\circ, 60^\circ$  and  $75^\circ$ , some joints close to the boundaries get truncated (Fig. 19(b)). The distance  $d$  shown in Figs. 19a and b is 3 cm. The results show that the ratio of jointed model strength to intact model strength decreases with increasing the ratio of joint length to rock bridge length.  $\beta=60^\circ, 30^\circ$  and  $45^\circ$  provide the highest effect on the said relation.  $\beta=90^\circ$  and  $75^\circ$  provide the lowest effect on the said relation. The moderate level effect on the mentioned relation can be seen for  $\beta=0^\circ$  and  $15^\circ$ . The ratio of jointed model strength to intact model strength shows values between 0.125 and 0.9. The conducted study shows that the ratio of the crack initiation stress of jointed model to intact model strength has an average value of about 0.48 with a variability of  $\pm 0.1$ . Ghazvinian *et al.* (2011) has investigated the failure mechanism of planar non-persistent open joints using PFC2D (Fig. 19(a)).

The joint length ( $b$ ) has a range from 12 to 25.5 mm with an increment of 4.5 mm, while the joint separation or ligament length ( $l$ ) decreases from 36 to 9 mm with a decrement value of 9 mm.

Results show that by increasing the joint coefficient, the most fractured surface changes to a single symmetrical failure surface. In all examined cases, about 45 % of the total number of cracks developed at the peak strength, and nearly 55 % of them developed after the peak shear resistance were reached. This revealed that, the models lost their loading capacities when 45 % of the total number of cracks developed within the rock bridge.

Sarfarazi *et al.* (2014) has investigated the Process of fracture of echelon rock joints using PFC2D (Fig 19(b)). Six ligament angles were investigated:  $0^\circ, 25^\circ, 50^\circ, 90^\circ, 115^\circ$  and  $140^\circ$ . The ligament lengths of 18 mm between the joints were kept constant for all models. For different ligament angles, the lengths of the edge-notched joints were different (i.e.  $b = 21, 21.8, 24.2, 33.8,$  and  $36.9$  mm for the ligament angles of  $0^\circ, 25^\circ, 50^\circ, 90^\circ, 115^\circ,$  and  $140^\circ$ , respectively). But in the same specimen, the lengths of those two edge joints were the same.

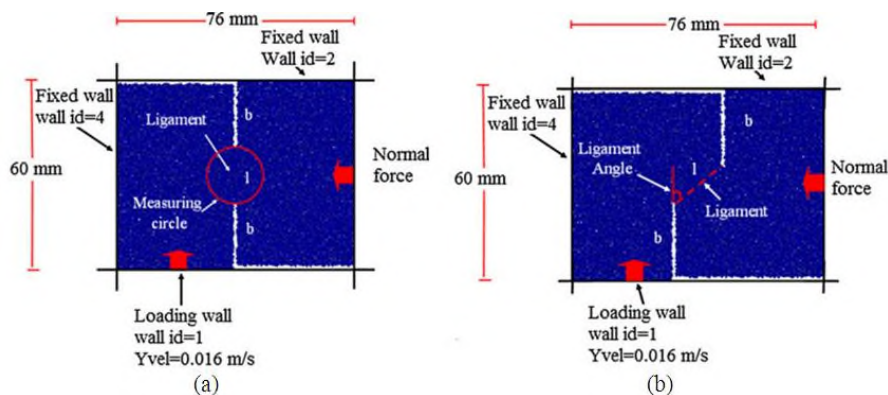


Fig. 19 (a) Planar non-persistent joints; Ghazvinian *et al.* (2011), (b) en-echelon non-persistent joints; Sarfarazi *et al.* (2014)

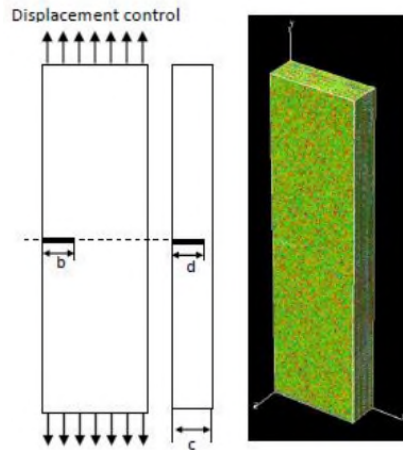


Fig. 20 Model consisting single joint

Results showed that, the failure pattern is highly dependent on joint overlapping. In non-overlapped joints, cracks were initiated from the joint tips and elliptical failure patterns occurred in the models. In overlapped joints, the cracks were initiated from the joint walls and a rectangular failure patterns occurred in the models. Joint configuration had also been shown to affect the shear strength of non-persistent joints, so the shear strength of non-overlapped joints was more than that of the overlapped joints.

The amount of fracturing at the peak shear loading stage decreased with increasing the rock bridge angle. This means that, the length of stable crack growth decreases with increasing ligament angle.

In non-overlapped joints, the crack initiation stress was less than the failure stress, so progressive failure occurs, whereas for overlapped joints the crack initiation stress was equal to failure stress, so brittle failure occurred.

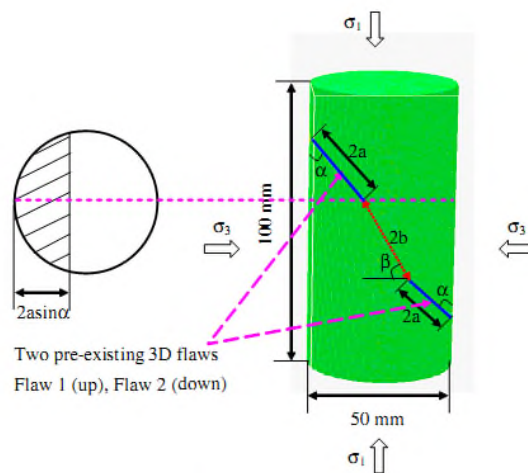


Fig. 21 Numerical model with two pre-existing 3D flaws

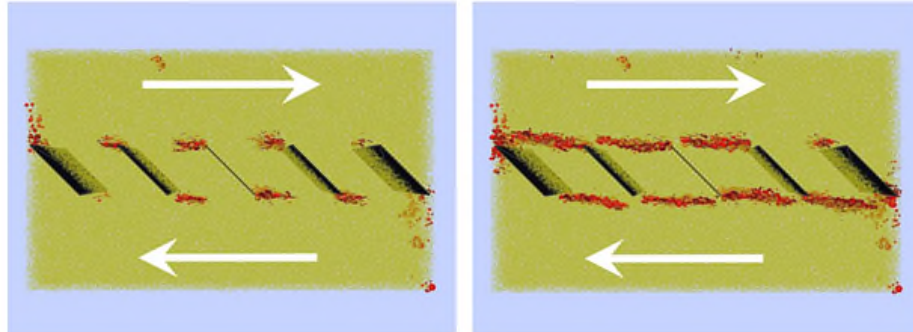


Fig. 22 Numerical prediction from the DEM

Wang *et al.* (2015) has investigated crack propagation of heterogeneous notched rock under uniaxial tension numerically (Fig. 20).

For the single-notched case, the numerical simulations reproduce the basic characteristics of the load-displacement curve of the fracture process zone. However, it is noted that after the peak stress, the development of the fracture process zone does not stop. Indeed, the post-peak stress stage contributes more to the development of the fracture process zone. In addition, with an increase of the length  $b$ , the peak stresses of the specimens decrease gradually while the residual strengths are almost the same. Moreover, 3D FPZs can be numerically simulated for the specimens with different internal depths. Although the surface FPZs look very similar, the failure modes for the specimens with varying thicknesses are quite different. This indicates that the 3D PRZs are very different to the two-dimensional ones.

Wang *et al.* (2014) has investigated failure behaviour of pre-cracked rock specimens under conventional triaxial compression using numerical method (Fig. 21) the numerical results show

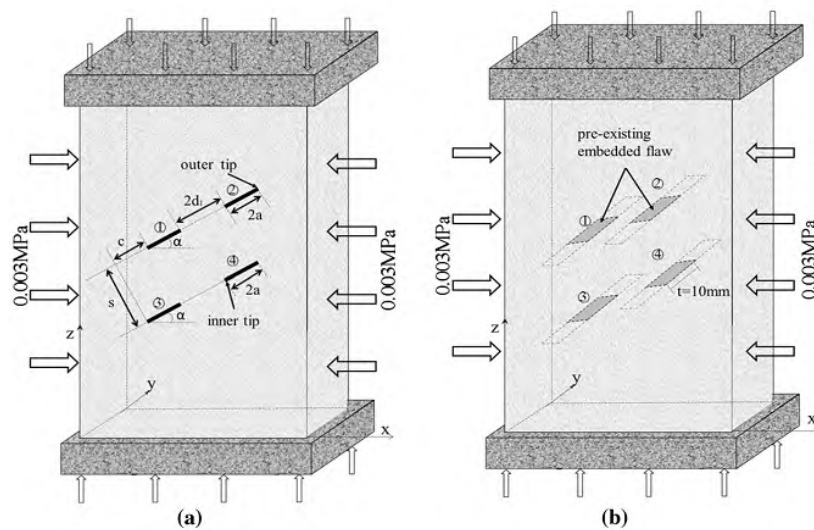


Fig. 23 The layout of samples containing four pre-existing flaws under biaxial compression: a the pre-existing penetrating flaws, b the pre-existing embedded flaws

that both the flaw angle and the ligament length can affect the final failure modes and the uniaxial compression strength of the rock specimen. The uniaxial compression strength increases slightly with increasing ligament angle. The uniaxial compression strength is the lowest when the flaw angle equals  $45^\circ$ . These numerical results are in agreement with the corresponding experimental results reported by Tien *et al.* (2006) and Wang *et al.* (2012b). Scholtes *et al.* (2012) has investigated the progressive failure in fractured rock masses using a 3D discrete element method (Fig. 22).

It is shown that the characteristic features of a fractured rock mass can be accurately modelled with the proposed approach. Particularly, the method is proven to reproduce the key mechanisms usually involved in the progressive failure of a jointed rock mass, i. e. deformation along pre-existing discontinuities, stress concentration at the discontinuity tips and the subsequent crack initiation and propagation (brittle fracturing) in the intact rock. The challenging wing crack extension, typical of brittle material fracturing, is successfully simulated under both compressive and shear loading, as a result of the progressive coalescence of local tensile micro-cracking. Bi *et al.* (2015) has done 3D Numerical Simulation for the Propagation Process of Multiple Pre-existing Flaws in Rock-Like Materials Subjected to Biaxial Compressive Loads (Fig. 23).

The results show that with increasing lateral stress, the secondary cracks keep growing in the samples, while the growth of the wing cracks is restrained. The main reason is that lateral stress hampers the growth of wing cracks. The samples subjected to biaxial compression are mainly split into fragments in a shear failure mode, which is different from a splitting failure of the samples subjected to uniaxial compression.

#### 4. Conclusions

The presence of rock bridges in not fully persistent natural discontinuity sets is a significant factor affecting the stability of rock structures. Compared with intact rocks, jointed rock masses are usually weaker, more deformable and highly anisotropic, depending upon the mechanical properties of each joint and the explicit joint positions.

Because of the inherent statistical nature and the uncertainties involved in the in situ survey of non-persistent joints, they are usually described by sets, hence by number of sets and the geometry of each set such as orientation, spacing and persistence. The fracture process of non-persistent joint can be divided into three main phases: The first phase of shearing is that of rock bridge rupture and model dilation, the second phase of shearing is characterized by friction processes and volume increase in the shear zone, finally, the third phase of shearing, reached after large shear displacements and determined by sliding processes inside the strongly fractured shear zone. These shear resistances corresponding to different shear mechanisms depend on various ways of testing conditions. Each can be the maximum shear resistance, so none of shear mechanisms may be neglected.

Researches show that, the bearing capacity of jointed rock decrease by increasing the number, the length and the inclination of non-persistent joint set. Coalescence in specimens with multiple flaws tends to occur in a ‘‘columnar’’ pattern where flaws in the same column are linked together. In fact the crack coalescence always occurs between the flaws for which the peak strength is lower.

The shear or mixed shear/tensile failure change to tensile failure by increasing the confining pressure, ligament length and ligament angle. Also, the bearing capacity of rock bridge increases

by increasing the confining pressure. It means that, when non-persistent joint is situated in shallow area, it suppressed by low confining pressure so tensile failure occurs in the rock bridge. For non-persistent joint located in deep area, shear failure occurs in the rock bridge.

## References

- Aliabadi, M.H. and Brebbia, C.A. (1993), "Advances in boundary element methods for fracture mechanics", *Amsterdam: Computational Mechanics Publications*, Elsevier.
- Altiero, N.Y. and Gioda, G. (1982), "An integral equation approach to fracture propagation in rock", *Riv. Ital. Geotecnica*, 387-404.
- Alzo'ubi (2001), "A fracture mechanisms of open offset rock joints under uniaxial loading", M. Sc. thesis, Jordan University of Science and Technology, Irbid, Jordan.
- Ashby, M.F. and Hallam, S.D. (1986), "The failure of brittle solids containing small cracks under compressive stress states", *Acta Metall.*, **34**(3), 497-510.
- Bahaaddini, M., Sharrock, G. and Hebblewhie, B.K. (2013), "Numerical investigation of the effect of joint geometrical parameters on the mechanical properties of a non-persistent jointed rock mass under uniaxial compression", *Comput. Geotech.*, **49**, 206-225.
- Batzle, M.L., Simmons, G. and Siegfried, R.W. (1980), "Microcrack closure in rocks under stress: direct observation", *J. Geophys. Res.*, **85**, 7072-90.
- Bi, J., Zhou, X.P. and Qian, Q.H. (2015), "The 3D numerical simulation for the propagation process of multiple pre-existing flaws in rock-like materials subjected to biaxial compressive loads", *Rock Mech. Rock Eng.*, (Published online).
- Bieniawski, Z.T. (1967), "Mechanism of brittle fracture of rock Part II-experimental studies", *Int. J. Rock Mech. Min. Sci. Geomech. Abstr.*, **4**, 407-23.
- Blandford, A.R., Ingraffea, A.R. and Liggett, J.A. (1981), "Two dimensional stress intensity factor computations using the boundary element method", *Int. J. Numer. Method. Eng.*, **17**(3), 387-401.
- Bobet, A. (1997), "Fracture coalescence in rock materials: experimental observations and numerical predictions", Sc.D. Thesis, MIT, Cambridge, USA.
- Bobet, A. (2000), "The initiation of secondary cracks in compression", *Eng. Fract. Mech.*, **66**(2), 187-219.
- Bobet, A. and Einstein, H.H. (1998), "Numerical modeling of fracture coalescence in rock materials", *Int. J. Fract.*, **92**(3), 221-52.
- Bobet, A. and Einstein, H.H. (1999), "Fracture coalescence in rock-type materials under uniaxial and biaxial compression", *Int. J. Rock Mech. Min. Sci.*, **35**(7), 863-889.
- Carpinteri, A. and Valente, S. (1988), "Size-scale transition from ductile to brittle failure: a dimensional analysis approach", *Proceedings of the CNRS-NSF, Workshop on strain localization and size effect due to cracking and damage*, Cachan, 447-90.
- Celestino, S.P., Piltner, R., Monteiro, P.J.M. and Ostertag, C.P. (2001), "Fracture mechanics of marble using a splitting tension test", *J. Mater. Civ. Eng.*, **13**(6), 407-411.
- Chen, G., Kemeny, J. and Harpalani, S. (1992), "Fracture propagation and coalescence in marble plates with pre-cut notches under compression", *Symp. on Fractured and Jointed Rock Mass, Lake Tahoe, CA*, 443-448.
- Chen, G., Zhang, Y., Huang, R., Guo, F. and Zhang, G. (2015), "Failure mechanism of rock bridge based on acoustic emission technique", *J. Sensors*, **15**, 1-10.
- Cheon, D., Jung, Y., Park, E., Song W. and Jang, H. (2011), "Evaluation of damage level for rock slopes using acoustic emission technique with waveguides", *Eng. Geol.*, **121** (1-2), 75-88.
- Cherepanov, G.P. (1966), "Propagation of cracks in compressed bodies", *J. Appl. Math. Mech.*, (English transl of Prikl Mate Mekh), **30**(1), 96-109.
- Committee on Fracture Characterization and Fluid Flow *et al.* (1996), "Rock fractures and fluid flow", Contemporary understanding and applications, Washington, DC: National Academic Press.

- De Bremaecker, J.C. and Ferris, M.C. (2004), "Numerical models of shear fracture propagation", *Eng. Fract. Mech.*, **71**(15), 2161-2178.
- Deng, Q. and Zhang, P. (1984), "Research on the geometry of shear fracture zones", *J. Geophys. Res.*, **89**(B7), 5669-5710.
- Dey, T.N. and Wang, C.Y. (1981), "Some mechanisms of microcrack growth and interaction in compressive rock failure", *Int. J. Rock Mech. Min. Sci. Geomech. Abstr.*, **18**(3), 199-209.
- Einstein, H.H., Veneziano, D., Baecher, G.B. and O'Reilly, K.J. (1983), "The effect of discontinuity persistence on rock slope stability", *Int. J. Rock Mech. Min. Sci. Geomech. Abstr.*, **20**(5), 227-36.
- Erdogan, F., Sih, G.C. (1963), "On the crack extension path in plates under plane loading and transverse shear", *ASMEJ Basic Eng.*, **85**(4), 516-27.
- Fredrich, J.T., Evans, B. and Wong, T.F. (1990), "Effect of grain size on brittle and semi brittle strength: Implications for micromechanical modelling of failure in compression", *J. Geophys. Res.*, **95**(B7), 10907-10920.
- Gehle, C. and Kutter, H.K. (2003), "Breakage and shear behavior of intermittent rock joints", *Int. J. Rock Mech. Min. Sci.*, **40**(5), 687-700.
- Germanovich, L.N., Carter, B.J., Dyskin, A.V., Ingraffea, A.R. and Lee, K.K. (1996), "Mechanics of 3-D crack growth under compressive loads. Rock mechanics tools and techniques", *Proceedings of the Second North American Rock Mechanics Symposium: NARMS '96. Rotterdam: Balkema*, 1151-1160.
- Ghazvinian, A., Nikudel, M.R. and Sarfarazi, V. (2007), "Effect of rock bridge continuity and area on shear behavior of joints", *Proceedings of the 11th congress of the international society of rock mechanics*, Lisbon, Portugal.
- Ghazvinian, A., Sarfarazi, V. and Moosavi, S.A. (2010), "Analysis of crack coalescence in rock bridges using neural network", *Proceedings of the European Rock Mechanics Symposium*, 255-258.
- Ghazvinian, A., Sarfarazi, V., Schubert, W. and Blumel, M.A. (2011), "Study of the failure mechanism of planar non-persistent open joints using PFC2D", *Rock Mech. Rock Eng. J.*, **45**(5), 677-693.
- Griffith, A.A. (1924), "The theory of rupture", *Proc. 1st Int. Congr. Appl. Mech. Delft*, 55-63.
- Griffith, A.A. (1921), "The phenomena of rupture and flow in solids", *Philos. Trans. R. Soc. London Ser. A*, **221**, 163 - 198.
- Haeri, H. (2015c), "Influence of the inclined edge notches on the shear-fracture behavior in edge-notched beam specimens", *Comput. Concrete*, **16**(4), 605-623.
- Haeri, H. (2015d), "Experimental crack analysis of rock-like CSCBD specimens using a higher order DDM", *Comput. Concrete*, **16**(6), 881-896.
- Haeri, H. (2015e), "Simulating the crack propagation mechanism of pre-cracked concrete specimens under shear loading conditions", *Strength Mater.*, **47**(4), 618-632.
- Haeri, H. (2015f), "Propagation mechanism of neighboring cracks in rock-like cylindrical specimens under uniaxial compression", *J. Min. Sci.*, **51**(3), 487-496.
- Haeri, H. and Marji, M.F. (2016b), "Simulating the crack propagation and cracks coalescence underneath TBM disc cutters", *Arab. J. Geosci.*, **9**(2), 1-10.
- Haeri, H. and Sarfarazi, V. (2016a), "The effect of micro pore on the characteristics of crack tip plastic zone in concrete", *Comput. Concrete*, **17**(1), 107-12.
- Haeri, H., Marji, M.F. and Shahriar, K. (2015b), "Simulating the effect of disc erosion in TBM disc cutters by a semi-infinite DDM", *Arab. J. Geosci.*, **8**(6), 3915-3927.
- Haeri, H., Marji, M.F., Shahriar, K. and Moarefvand, P. (2014a), "On the strength and crack propagation process of the pre-cracked rock-like specimens under uniaxial compression", *Strength Mater.*, **46**(1), 171-185.
- Haeri, H., Marji, M.F., Shahriar, K. and Moarefvand, P. (2014b), "On the crack propagation analysis of rock like Brazilian disc specimens containing cracks under compressive line loading", *Latin American J. Solid. Struct.*, **11**(8), 1400-1416.
- Haeri, H., Marji, M.F., Shahriar, K. and Moarefvand, P. (2014c), "A coupled numerical-experimental study of the breakage process of brittle substances", *Arab. J. Geosci.*, **8**(2), 809-825
- Haeri, H., Marji, M.F., Shahriar, K. and Moarefvand, P. (2014d), "On the cracks coalescence mechanism

- and cracks propagation paths in rock-like specimens containing pre-existing random cracks under compression”, *J. Central S. Univ.*, **21**(6), 2404-2414.
- Haeri, H., Marji, M.F., Shahriar, K. and Moarefvand, P. (2014e), “Investigating the fracturing process of rock-like Brazilian discs containing three parallel cracks under compressive line loading”, *Strength Mater.*, **46**(3), 133-148
- Haeri, H., Marji, M.F., Shahriar, K. and Moarefvand, P. (2014f), “Experimental and numerical study of crack propagation and coalescence in pre-cracked rock-like disks”, *Int. J. Rock Mech. Min. Sci.*, **67**, 20-28.
- Haeri, H., Marji, M.F., Shahriar, K. and Moarefvand, P. (2015a), “On the HDD analysis of micro cracks initiation, propagation and coalescence in brittle substances”, *Arab. J. Geosci.*, **8**(5), 2841-2852.
- Hall, S.A., De Sanctis, F. and Viggiani, G. (2006), “Monitoring fracture propagation in a soft rock (Neapolitan Tuff) using acoustic emissions and digital images”, *Pure Appl. Geophys.*, **163**(10), 2171-2204.
- Hallbauer, D.K., Wagner, H.N.G.W. and Cook, N.G.W. (1973), “Some observations concerning the microscopic and mechanical behaviour of quartzite specimens in stiff, triaxial compression tests”, *Int. J. Rock Mech. Min. Sci. Geomech. Abstr.*, **10**(6), 713-726.
- Hoek, E. and Bieniawski, Z.T. (1984), “Brittle fracture propagation in rock under compression”, *Int. J. Fract.*, **26**(4), 276-294.
- Horii, H. and Nemat-Nasser, S. (1985), “Compression-induced microcrack growth in brittle solids: axial splitting and shear failure”, *J. Geophys. Res.*, **90**(B4), 3.
- Horii, S. and Nemat-Nasser, S. (1986), “Brittle failure in compression: splitting, faulting and brittle-ductile transition”, *Phil. Trans. R. Soc. Lond.*, **319**(1549), 337-74.
- Hu, B., Zhang, N. and Liu, S. (2009), “Contrastive model test for joint influence on strength and deformation of rock masses”, *J. Central S. Univ. (Sci. Tech.)*, **40**, 1133-1138.
- Hussain, M.A. and Pu, E.L. (1974), “Underwood JH, Strain energy release rate for a crack under combined model I and mode II”, **560**, 2-28.
- Ibraheem, O.F., Bakar, B.H.A. and Johari, I. (2015), “Behavior and crack development of fiber-reinforced concrete spandrel beams under combined loading: an experimental study”, *Struct. Eng. Mech.*, **54**(1), 1-17.
- Ingraffea, A.R. and Heuze, F.E. (1980), “Finite element models for rock fracture mechanics”, *Int. J. Numer. Anal. Meth. Geomech.*, **4**(1), 25-43.
- Irwin, G.R. (1957), “Analysis of stresses and strains near the ends of a crack traversing a plate”, *J. Appl. Mech.*, **24**, 361-364.
- Jaeger, J.C. (1971), “Friction of rocks and stability of rock slopes”, *Geotech.*, **21**(2), 97-134.
- Jamil, S.M. (1999), “Strength of non-persistent rock joints”, Ph. D. thesis, University of Illinois at Urbana-Champaign, IL, U.S.A.
- Jansen, D.P., Carlson, S.R., Young, R.P., and Hutchins, D.A. (1993), “Ultrasonic imaging and acoustic emission monitoring of thermally induced microcracks in Lac du Bonnet granite”, *J. Geophys. Res. Solid Earth*, **98**(B12), 22231-22243.
- Jennings, J.E. (1970), “A mathematical theory for the calculation of the stability of slopes in open cast mines”, *Planning Open Pit Mines, Proceedings of the Symposium on the Theoretical Background to the Plannings of Open Pit Mines with Special Reference to Slope Stability*, Johannesburg, 87-102.
- Jiefan, H., Ganglin, C., Yonghong, Z. and Ren, W. (1990), “An experimental study of the strain field development prior to failure of a marble plate under compression.”, *Tectonophys.*, **175**(6), 269-284.
- Kemeny, J. (2005), “Time-dependent drift degradation due to the progressive failure of rock bridges along discontinuities”, *Int. J. Rock Mech. Min. Sci.*, **42**(1), 35-46.
- Kemeny, J.M. (1991), “A model for non-linear rock deformation under compression due to subcritical crack growth”, *Int. J. Rock Mech. Min. Sci. Geomech. Abstr.*, **28**(3), 459-467.
- Kemeny, J.M. and Cook, N.G.W. (1987), “Crack models for the failure of rock under compression”, *Proc. 2nd Int. Conf. Constitutive Laws for Eng. Materials*, **2**, 879-887.
- Kranz, R.L. (1979), “Crack-crack and crack-pore interaction s in stressed granite”, *Int. J. Rock Mech. Min.*

- Sci. Geomech. Abstr.*, **16**, 37- 47.
- Kranz, R.L., Microcracks in rocks: A review. *Tectonophysics* , 1983, 100, 449 - 480.
- Kulatilake, P.H.S.W., Malama, B. and Wang, J. (2001), "Physical and particle flow modeling of jointed rock block behaviour under uniaxial loading", *Int. J. Rock Mech. Min. Sci.*, **38**(5), 641-657.
- Kuntz, M. and Lavallee, P. (1998), "Steady-state flow experiments to visualise the stress field and potential crack trajectories in 2D elastic-brittle cracked media in uniaxial compression", *Int. J. Fract.*, **92**(4), 349-357.
- Lajtai, E.Z. (1969b), "Shear strength of weakness planes in rock", *Int. J. Rock Mech. Min. Sci.*, **6**(5), 499-515.
- Lajtai, E.Z.(1969a), "Strength of discontinuous rocks in direct shear", *Geotech.*, **19**(2), 218-332.
- Li, C., Stephansson, O. and Savilahti, T. (1990), "Behavior of rock joints and rock bridges in shear testing", *Proceedings of the International Symposium on Rock Joints*, 259-266.
- Li, Y., Chen, L. and Wang, Y. (2005), "Experimental research on pre-cracked marble under compression", *Int. J. Solid. Struct.*, **42**(9), 2505-2516.
- Li, Y.P. and Wang, Y.H. (2003), "Analysis on zigzag cracks in rock-like materials under compression", *Acta Mech. Solida Sinica*, **24**(4), 456-462.
- Lin, P., Wong, R.H.C., Chau, K.T. and Tang, C.A. (2000), "Multi-crack coalescence in rock-like material under uniaxial and biaxial loading", *Key Eng. Mater.*, **183**, 809-14.
- Liu, H.Y., Kou, S.Q., Lindqvist, P.A. and Tang, C.A. (2004), "Numerical simulation of shear fracture (mode II) in heterogeneous brittle rock", *Int. J. Rock Mech. Min. Sci.*, **41**, 3.
- Mao, H. and Yang, C. (2009), "Analysis of deformation features of slates with structural surfaces", *Chinese J. Underg. Space Eng.*, **5**, 934-938.
- Mingli, H., Chunan, T. and Wancheng, Z. (1999), "Real-time SEM study on rock failure instability under uniaxial compression", *J. Northeastern Univ. Natural Sci.*, **20**, 429-432.
- Mughieda, O. and Alzoubi, A. (2004), "Fracture mechanisms of offset rock joints-A laboratory investigation", *Geotech. Geol. Eng.*, **22**, 545-562.
- Mughieda, O. and Karasneh, I. (2006), "Coalescence of offset rock joints under", *Geotech. Geol. Eng.*, **24**, 985-999.
- Mughieda, O. and Omar, M.T. (2008), "Stress analysis for rock mass failure with offset joints", *Geotech. Geol. Eng.*, **26**(5), 543-552.
- Mughieda, V. and Khawaldeh, I. (2004), *Scale effect on engineering properties of open non-persistent rock joints under uniaxial loading*, *Bölgesel Kaya Mekaniği i Sempozyumu/ ROCKMEC '2004-VIIth Regional Rock Mechanics Symposium*, Sivas, Türkiye.
- Nemat-Nasser, S. and Horii, H. (1982), "Compression-induced non-planar crack extension with application to splitting, exfoliation and rockburst", *J. Geophys. Res.*, **87**(B8), 6805-6821.
- Olsson, W.A. and Pang, S.S. (1976), "Microcrack nucleation in marble", *Int. J. Rock Mech. Min. Sci. Geomech. Abstr.*, **13**(2), 53- 59.
- Pan, B., Gao, Y. and Zhong, Y. (2014), "Theoretical analysis of overlay resisting crack propagation in old cement concrete pavement", *Struct. Eng. Mech.*, **52**(4), 829-841.
- Papadopoulos, G.A. and Poniridis, P.I. (1989), "Crack initiation under biaxial loading with higher-order approximation", *Eng. Fract. Mech.*, **32**(3), 351-360.
- Peng, S. and Johnson, A.M. (1972), "Crack growth and faulting in cylindrical specimens of Chelmsford granite", *Int. J. Rock Mech. Min. Sci. Geomech. Abstr.*, **9**(1), 37-86, Pergamon.
- Petit, J. P. and Barquins, M. (1988), "Can natural faults propagate under mode II conditions?", *Tecton.*, **7**(6), 1243-1256.
- Potyondy, D.O. and Cundall, P.A. (2004), "A bonded-particle model for rock", *Int. J. Rock Mech. Min. Sci.*, **41**(8), 1329-1364.
- Prudencio, M. and Van Sint Jan, M. (2007), "Strength and failure modes of rock mass models with non-persistent joints", *Int. J. Rock Mech. Min. Sci.*, **44**(6), 890-902.
- Pu, C.Z., Cao, P., Zhao Y.L., Zhang, X.Y., Yi, Y.L. and Lit, Y.K. (2010), "Numerical analysis and strength experiment of rock-like materials with multi-fissures under uniaxial compression", *J. Rock Soil Mech.*, **11**,

051.

- Reyes, O. (1991), "Experimental study, analytic modeling of compressive fracture in brittle materials", Ph.D.Thesis, Massachusetts Institute of Technology, Cambridge.
- Reyes, O. and Einstein, H.H. (1991), "Failure mechanism of fractured rock fracture coalescence model", *Proceeding of the Seventh Congress of the ISRM*, **I**, 333-40.
- Rudajev, V., Vilhelm, J. and Lokajiček, T. (2000), "Laboratory studies of acoustic emission prior to uniaxial compressive rock failure", *Int. J. Rock Mech. Min. Sci.*, **37**(4), 699-704.
- Sagong, M. and Bobet, A. (2000), "Coalescence of multiple flaws in uniaxial compression", *Proceedings of the North American Rock Mechanics Symposium: Pacific Rocks*, 1203-1210.
- Sagong, M. and Bobet, A. (2002), "Coalescence of multiple flaws in a rock-model material in uniaxial compression", *Int. J. Rock Mech. Min. Sci.*, **39**(2), 229-241.
- Sammis, C.G. and Ashby, M.F. (1986), "The failure of brittle porous solids under compressive stress states", *Acta Metall.*, **34**(3), 511-526.
- Sarfarazi, V., Ghazvinian, A., Schubert, W., Blumel, M. and Nejati, H.R. (2014), "Numerical simulation of the process of fracture of Echelon rock joints", *Rock Mech. Rock Eng.*, **45**(5), 677-693.
- Savilahti, T., Nordlund, E. and Stephansson, O. (1990), "Shear box testing and modeling of joint bridge", *Proceedings of international symposium on shear box testing and modeling of joint bridge Rock Joints*, 295-300, Norway.
- Scavia, C. (1999), "The displacement discontinuity method for the analysis of rock structures: a fracture mechanic", *Aliabadi MH, editor. Fracture of Rock. Boston: WIT press, Computational Mechanics Publications*, 39-82.
- Scavia, C. and Castelli, M. (1996), "Analysis of the propagation of natural discontinuities in rock bridges", Barla G, ed. EUROCK'98. Rotterdam: Balkema, 445-51.
- Scholtes, L. and Donze, F. (2012), "Modelling progressive failure in fractured rock masses using a 3D discrete element method", *Int. J. Rock Mech. Min. Sci.*, **52**(2012), 18-30.
- Shah, S.P. (1999a), "Fracture toughness for high-strength concrete", *ACI Mater.*, **87**, 260-265.
- Shah, S.P. (1999b), "Experimental methods for determining fracture process zone and fracture parameters", *Eng. Fract. Mech.*, **35**, 3-14.
- Shang, J.L., Kong, C.J., Li, T.J. and Zhang, W.Y. (1999), "Observation and study on meso-damage and fracture of rock", *J. Exp. Mech.*, **14**, 373-383.
- Shen, B. (1993), "The mechanics of fracture coalescence in compression experimental study and numerical simulation", *Eng. Fract. Mech.*, **51**(1), 73-85.
- Shen, B. and Stephansson, O. (1990), "Cyclic loading characteristics of joints and rock bridges in a jointed rock specimen", *Proceedings of the International Symposium on Rock Joints*, 725-729.
- Shen, B. and Stephansson, O. (1994), "Modification of the g-criterion for crack propagation subjected to compression", *Eng. Fract. Mech.*, **47**(2), 177-89.
- Shen, B., Stephansson, O., Einstein, H.H. and Ghahreman, B. (1995), "Coalescence of fracture under shear stresses in experiments", *J. Geophys. Res.*, **100**, 725-729.
- Sih, G.C. (1974), "Strain-energy-density factor applied to mixed mode crack problems", *Int. J. Fract.*, **10**(3), 305-321.
- Steif, P.S. (1984), "Crack extension under compressive loading", *Eng. Fract. Mech.*, **20**(3), 463-473.
- Stimpson, B. (1978), "Failure of slopes containing discontinuous planar joints", *Proceedings of the 19th US Symposium on Rock Mechanics*, Stateline, Nevada, 296-302.
- Takeuchi, K. (1991), "Mixed-mode fracture initiation in granular brittle materials", M.S. Thesis, Massachusetts Institute of Technology, Cambridge, MA.
- Tang, C. (1997), "Numerical simulation of progressive rock failure and associated seismicity", *Int. J. Rock Mech. Min. Sci.*, **34**(2), 249-261.
- Tang, C.A. and Kou, S.Q. (1998), "Crack propagation and coalescence in brittle materials under compression", *Eng. Fract. Mech.*, **61**(3), 311-324.
- Tang, C.A. and Kou, S.Q. (1998), "Fracture propagation and coalescence in brittle materials", *Eng. Fract. Mech.*, **61**(3), 311-324.

- Tapponnier, P. and Brace, W.F. (1976), "Development of stress-induced micro-cracks in Westerly granite", *Int. J. Rock Mech. Min. Sci. Geomech. Abstr.*, **13**(4), 103-12.
- Tien, Y.M., Kuo, M.C. and Juang, C.H. (2006), "An experimental investigation of the failure mechanism of simulated transversely isotropic rocks", *Int. J. Rock Mech. Min. Sci.*, **43**(8), 1163-1181.
- Vasarhelyi, B. and Bobet, A. (2000), "Modeling of crack initiation, propagation and coalescence in uniaxial compression", *Rock Mech. Rock Eng.*, **33**(2), 119-39.
- Wang, S., Huang, R., Ni, P., Gamage, R.P. and Zhang, M. (2013), "Fracture behavior of intact rock using acoustic emission: experimental observation and realistic modeling", *Geotech. Test. J.*, **36**(6), 1-12.
- Wang, S.Y., Sloan, S.W., Sheng, D.C. and Tang, C.A. (2015), "3D numerical analysis of crack propagation of heterogeneous notched rock under uniaxial tension", *Tectonophys.*, **16**, 30042-7.
- Wang, S.Y., Sloan, S.W., Sheng, D.C., Yang, S.Q. and Tang, C.A. (2014), "Numerical study of failure behaviour of pre-cracked rock specimens under conventional triaxial compression", *Int. J. Solid. Struct.*, **51**(5), 1132-1148.
- Wang, S.Y., Sloan, S.W., Tang, C.A. and Zhu, W.C. (2012b), "A numerical investigation of the failure mechanism around tunnels in transversely isotropic rock masses", *Tunnel. Underg. Space Tech.*, **32**, 231-244.
- Wong, R.H.C., Chau, K.T., Tsoi, P.M. and Tang, C.A. (1999), "Pattern of coalescence of rock bridge between two joints under shear testing", *Proceedings of the 9th International Congress on Rock Mechanics*, 735-738.
- Wong, R.H.C. (1997), "Failure mechanisms, peak strength of natural rocks and rock-like solids containing frictional cracks", Ph.D. Thesis, The Hong Kong Polytechnic University, Hong Kong.
- Wong, R.H.C. and Chau, K.T. (1997), "The coalescence of frictional cracks and the shear zone formation in brittle solids under compressive stresses", *Int. J. Rock Mech. Min. Sci.*, **34**(3), 366.
- Wong, R.H.C. and Chau, K.T. (1998), "Crack coalescence in a rock-like material containing two cracks", *Int. J. Rock Mech. Min. Sci.*, **35**(2), 147-164.
- Wong, R.H.C. and Chau, K.T. (1998), "Peak strength of replicated and real rocks containing cracks", *Key Eng. Mater.*, **145**, 953-8.
- Wong, R.H.C., Chau, K.T., Tang, C.A. and Lin, P. (2001), "Analysis of crack coalescence in rock-like materials containing three flaws-part I: experimental approach", *Int. J. Rock Mech. Min. Sci.*, **38**(7), 909-924.
- Wong, R.H.C., Chau, K.T., Tang, C.A. and Lin, P. (2001), "Analysis of crack coalescence in rock-like materials containing three flaws-Part I: experimental approach", *Int. J. Rock Mech. Min. Sci.*, **38**, 909-24.
- Wong, R.H.C., Leung, W.L. and Wang, S.W. (2001), "Shear strength study on rock-like models containing arrayed open joints. Rock mechanics in the national interest", Elsworth D, Tinucci JP, Heasley KA, Eds. Swets & Zeitlinger Lisse, 843-9.
- Wong, R.H.C., Lin, P., Chau, K.T. and Tang, C.A. (2000), "The effects of confining compression on fracture coalescence in rock-like material", *Key Eng. Mater.*, **183**, 857-62.
- Wong, R.H.C., Lin, P., Tang, C.A. and Chau, K.T. (2002), "Creeping damage around an opening in rock-like material containing non-persistent joints", *Eng. Fract. Mech.*, **69**(17), 2015-2027.
- Wong, R.H.C., Tang, C.A., Chau, K.T. and Lin, P. (2002), "Splitting failure in brittle rocks containing pre-existing flaws under uniaxial compression", *Eng. Fract. Mech.*, **69**(17), 1853-1871.
- Wong, T.F. (1982), "Micromechanics of faulting in Westerly granite", *Int. J. Rock Mech. Min. Sci. Geomech. Abstr.*, **19**(2), 49- 64.
- Xiang, F., Kulailake, P.H.S.W., Xin, C. and Ping, C. (2015), "Crack initiation stress and strain of jointed rock containing multi-cracks under uniaxial compressive loading: A particle flow code approach", *J. Cent. South Univ.*, **22**(2), 638-645.
- Yang, S., Jing, H. and Wang, S. (2012), "Experimental investigation on the strength, deformability, failure behaviour and acoustic emission locations of red sandstone under triaxial compression", *Rock Mech. Rock Eng.*, **45**(4), 583-606.
- Yin, L. and Zhang, P. (2010), "Simulation analysis of rock mass strength affected by dual structural plane", *J. Min. Safety Eng.*, **4**, 600-603.

- Zhang, F., Wang, B., Chen, Z., Wang, X. and Jia, Z. (2008), "Rock bridge slice element method in slope stability analysis based on multi-scale geological structure mapping", *J. Cent. S. Univ. Tech.*, **15**(2), 131-137.
- Zhang, H.Q., Zhao, Z.Y., Tang, C.A. and Song, L. (2006), "Numerical study of shear behavior of intermittent rock joints with different geometrical parameters", *Int. J. Rock Mech. Min. Sci.*, **43**(5), 802-816.
- Zhang, X. and Wong, R.H.C. (2013), "Crack initiation, propagation and coalescence in rock-like material containing two flaws: A numerical study based on bonded-particle model approach", *J. Rock Mech. Rock Eng.*, **46**(5), 1001-1021.
- Zhang, X., Wong, L.N.Y. (2012), "Cracking process in rock-like material containing a single flaw under uniaxial compression: A numerical study based on parallel bonded-particle model approach", *Rock Mech. Rock Eng.*, **45**(5), 711-737.
- Zhao, Y. and Wan, W. (2013), "An experimental and simulation analysis on fracture of rock bridge under shear pressure", **18**, 419-426.
- Zhao, Y.H., Liang, H.H., Huang, J.F., Geng, J.D. and Wang, R. (1995), "Development of sub cracks between en echelon fractures in rock plates", *Pure Appl. Geophys.*, **145**, 759-73.
- Zhu, W., Li, S., Wong, R.H.C., Chau, K.T. and Xu, J. (2004), "A study of fracture mechanism and shear strength of rock bridges through analytical and model-testing methods", *Key Eng. Mater.*, **261-263**, 225-230.
- Zhu, W.S., Chen, W.Z. and Shen, J. (1998), "Simulation experiment and fracture mechanism study on propagation of Echelon pattern cracks", *Acta Mech. Solida Sinica*, **19**, 355-360.